Journal of Complex Networks (2021) **0**, 1–39
doi: 10.1093/comnet/cnab032

Review

Random walks on weighted networks: a survey of local and non-local dynamics

A. P. Riascos[†]

Instituto de Física,Universidad Nacional Autónoma de México, Apartado Postal 20-364, 01000 Ciudad de México, México

[†]Corresponding author. Email: aperezr@fisica.unam.mx

AND

José L. Mateos

Instituto de Física,Universidad Nacional Autónoma de México, Apartado Postal 20-364, 01000 Ciudad de México, México and Centro de Ciencias de la Complejidad, Universidad Nacional Autónoma de México, Apartado Postal 04510, Ciudad de México, México

Edited by: Ernesto Estrada

[Received on 27 May 2021; editorial decision on 1 September 2021; accepted on 6 September 2021]

In this article, we present a survey of different types of random walk models with local and non-local transitions on undirected weighted networks. We present a general approach by defining the dynamics as a discrete-time Markovian process with transition probabilities expressed in terms of a symmetric matrix of weights. In the first part, we describe the matrices of weights that define local random walk dynamics like the normal random walk, biased random walks and preferential navigation, random walks in the context of digital image processing and maximum entropy random walks. In addition, we explore non-local random walks, like Lévy flights on networks, fractional transport through the new formalism of fractional graph Laplacians, and applications in the context of human mobility. Explicit relations for the stationary probability distribution, the mean first passage time and global times to characterize random walks are obtained in terms of the elements of the matrix of weights and its respective eigenvalues and eigenvectors. Finally, we apply the results to the analysis of particular local and non-local random walk dynamics, and we discuss their capacity to explore several types of networks. Our results allow us to study and compare the global dynamics of different types of random walk models.

Keywords: random walks; networks; diffusion; Lévy flights.

1. Introduction

Since their introduction as an informal question posted in the journal Nature in 1905 by Rayleigh, random walks have had an important impact in science with applications in a broad range of fields like mathematics, biology, physics, chemistry, economics, finance, among many others [1, 2]. The success of random walk models in different applications lies in their simplicity and generality. Typically, it is defined as a walker in a particular space that moves randomly, making this characteristic a good candidate in the description of processes like diffusive transport, chemical reactions, fluctuations in the economy and even in the foraging of some animal species [1–7]. Despite the mentioned simplicity in the definition,

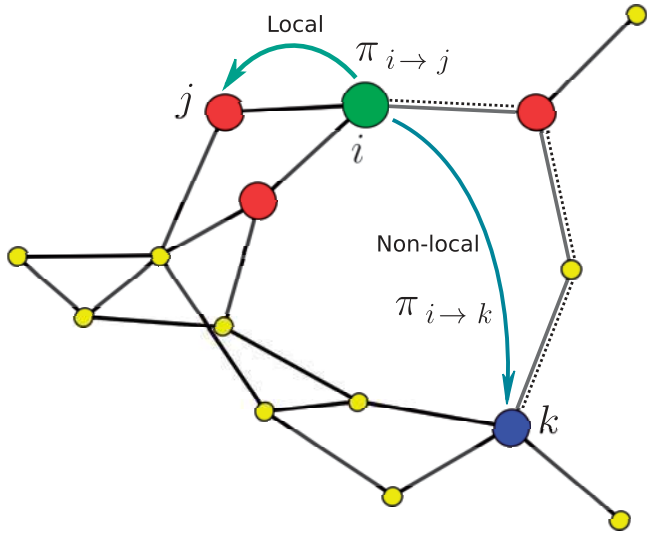

FIG. 1. Two types of transitions of a random walker on a network. The walker can hop from i to the node j that is one of the three nearest-neighbours available for a local transition. Also can make a non-local transition to reach the node k. In the non-local displacement, the length of the shortest path is three as indicated by the dashed line.

the consequences of the dynamics of a random walker are non-trivial and continue to surprise us with new results and with all the complexity that emerges from its simple rules.

In recent years, much of the interest in random walks have migrated to the study of complex systems described through networks [8–13]. In this context, the interplay between the topology of the network and the dynamical processes taking place on this structure are of utmost importance [13–15]. In particular, random walk models that allow transitions from one node to one of its nearest neighbours on the network constitutes a paradigmatic case and are the natural framework to study diffusive transport [14, 16–18], navigation and search processes in networks [19–22], multiplex networks [23], with applications in a variety of systems like the propagation of epidemics and spreading phenomena [24, 25], the dynamics on social networks [26], the analysis of information [27], human mobility [28, 29], among others [2, 14].

On the other hand, in different cases full or partial knowledge of the network structure is available to define a random walk capable of using this information to increase the capacity to visit nodes with hops to the nearest neighbours but also long-range transitions beyond this local neighbourhood. In Fig. 1, we illustrate local and non-local transitions in a network. In this case, the walker can visit one of the nearest-neighbours with a local transition, but there is also the possibility of a non-local transition. By using this long-range dynamics the random walker can directly contact long-distance nodes without the intervention of intermediate nodes and without altering the topology of the network. As we will see, some non-local random walk models consider the shortest path connecting two nodes whereas others include quantities that contain all the possible paths between nodes.

In addition, random walks with a non-local character have been explored in the literature. This is the case of Lévy flights on networks where random transitions occur to non-nearest neighbours with a probability that decays as a power law of the distance separating two nodes [30]; the capacity of this dynamical process to explore networks has been studied in Refs. [30–36]. Lévy flights on networks were generalized by Estrada *et al.* by using a random multi-hopper model defined in terms of decaying functions of the shortest-path distances; this approach is explored in detail in Ref. [37]. Furthermore, we also found non-local hops in the fractional transport on networks defined in terms of the fractional

graph Laplacian [39]. In this case, long-range displacements on the network emerge from a formalism that was introduced as the equivalent on networks of the fractional diffusion equation in the continuum [39, 40]. This model is studied in the context of transport on networks and lattices [39–48], in connection with information analysis [49–51], quantum transport on networks [52], random walks on networks with stochastic resetting [53, 54] and fractional diffusion in the context of COVID-19 [55]. The fractional transport is a particular case of a series of dynamics that can be defined in terms of functions of the Laplacian of a network [56]. In general, the study of random walks with long-range displacements on networks opens several questions regarding the way in which these large displacements can appear or be induced in different applications.

In this article, we present a survey of different types of local and non-local random walks on networks. We describe a general approach to study these processes using the information contained in a symmetric matrix of weights used to define the probability of transition between nodes. We model the dynamics as a discrete time Markovian process. In the first part, we describe the matrices of weights that define local random walks: traditional random walks, biased random walks, random walks in the context of digital image processing and maximum entropy random walks. In the same way, examples of non-local random walks are described: Lévy flights on networks, fractional transport and applications in the context of human mobility. In all these cases, explicit relations for the stationary probability distribution of the random walker are obtained in terms of the elements of the matrix of weights that defines each model. After analysing the transition matrix for these different processes, in a second part of the article, a general formalism to calculate the mean first passage time and global times to characterize the dynamics is presented. Analytical expressions in terms of eigenvalues and eigenvectors of the transition matrix are obtained for all these quantities. Finally, we apply the results to the analysis of local and non-local random walks to discuss and compare their capacity to explore networks.

2. Random walks on weighted networks

In this section, we introduce different concepts about random walks on weighted networks and the notation implemented to describe this process. We introduce a general random walker with transition probabilities in a network and a matrix of weights; the respective temporal evolution is modelled as a discrete time Markovian process for which we find an analytical result for its stationary probability distribution.

We consider undirected weighted networks with N nodes $i = 1, \ldots, N$. The topology of the network is described by an adjacency matrix $\mathbf{A}$ with elements $A_{ij} = A_{ji} = 1$ if there is an edge between the nodes i and j and $A_{ij} = 0$ otherwise; in particular, we consider throughout this article that $A_{ii} = 0$ to avoid loops connecting a node with itself. The degree of the node i is the number of neighbours that this node has and is given by $k_i = \sum_{l=1}^{N} A_{il}$. Additionally to the network structure, we have a $N \times N$ symmetric matrix of weights Ω with elements $\Omega_{ij} = \Omega_{ji} \geq 0$ and $\Omega_{ii} = 0$. The matrix Ω can include information of the structure of the network or incorporate additional data describing characteristics of links and nodes. By definition, the strength of the node i is given by $S_i = \sum_{l=1}^{N} \Omega_{il}$ and represents the total weight of the node i, also called '*weighted degree*' or '*node strength*'.

In the following, we study discrete time random walks on connected weighted networks with transition probabilities between nodes determined by the elements of the matrix of weights Ω. The occupation probability to find the random walker in the node j at time t, starting from i at $t = 0$, is given by $P_{ij}(t)$ and obeys the master equation [7, 16]

$$P_{ij}(t+1) = \sum_{m=1}^{N} P_{im}(t)\pi_{m\to j}\,, \tag{2.1}$$

where the transition probability $\pi_{i\to j}$ between the nodes i and j is given by

$$\pi_{i\to j} = \frac{\Omega_{ij}}{\sum_{l=1}^{N}\Omega_{il}} = \frac{\Omega_{ij}}{S_i}. \tag{2.2}$$

The transition matrix Π, with elements $\pi_{i\to j}$, in the general case is not symmetric; however, as a consequence of Eq. (2.2) and the symmetry of the matrix Ω, we obtain $S_i\pi_{i\to j} = S_j\pi_{j\to i}$, a result that establishes a connection between the transition probabilities $\pi_{i\to j}$ and $\pi_{j\to i}$. On the other hand, iterating the master equation (2.1), the probability $P_{ij}(t)$ takes the form

$$P_{ij}(t) = \sum_{j_1,\cdots,j_{t-1}} \pi_{i\to j_1}\cdot\pi_{j_1\to j_2}\cdots\pi_{j_{t-1}\to j} \tag{2.3}$$

and, using Eq. (2.3), we obtain

$$\begin{aligned} P_{ij}(t) &= \sum_{j_1,\cdots,j_{t-1}} \frac{S_{j_1}}{S_i}\cdots\frac{S_j}{S_{j_{t-1}}}\pi_{j\to j_{t-1}}\cdots\pi_{j_1\to i} \\ &= \frac{S_j}{S_i}P_{ji}(t). \end{aligned} \tag{2.4}$$

In this way, the detailed balance condition

$$S_iP_{ij}(t) = S_jP_{ji}(t) \tag{2.5}$$

is deduced as a direct consequence of the symmetry of Ω. The relation in Eq. (2.5) allows to obtain the stationary probability distribution $P_j^{\infty} = \lim_{t\to\infty}P_{ij}(t)$, that gives the probability to find the random walker in the node j when $t\to\infty$. We have

$$P_i^{\infty} = \frac{S_i}{\sum_{l=1}^{N}S_l}, \tag{2.6}$$

showing that the stationary distribution P_i^{∞} of the node i is directly proportional to its strength S_i. The stationary distribution P_i^{∞} in Eq. (2.6) is a general result that characterizes the global behaviour of the random walker. As we will see in the next section, this quantity allows to rank and classify the nodes of the network with a measure that combines the topological characteristics of the network structure with their capacity of transport modelled by the master equation (2.1) and the transition matrix Π. Furthermore, it is well known in the context of Markovian processes that the value $1/P_i^{\infty}$ is the average number of steps required for the random walker to return for the first time to the node i [57, 58]. Diverse types of random walk models can be explored in terms of the matrix of weights formalism described before. The only restrictions to this approach are the symmetry of the elements of the matrix of weights $\Omega_{ij} = \Omega_{ji}$, the condition $\Omega_{ij}\geq 0$ and $\Omega_{ii} = 0$. In the following, we present particular cases of random walk models that can be described by using this method. We divide our discussion into local models, for which the transitions of the random walker are restricted to adjacent sites on the network, and long-range models, for which the walker can hop with displacements beyond its nearest neighbours.

3. Local random walk models

In local random walk models, the random walker always hops from a node to one of its nearest neighbours on the network. As a consequence, the elements of the matrix of weights take the form $\Omega_{ij} = g_{ij}A_{ij}$, where, as we explain in the following part, the value g_{ij} is related to quantities assigned to each node or to the weight of the link that connects the nodes i and j.

3.1 *Normal random walk*

In this case, the weights coincide with the elements of the adjacency matrix; therefore $\Omega_{ij} = A_{ij}$. As a consequence, from Eq. (2.2), the transition matrix is given by [21]

$$\pi_{i\to j} = \frac{A_{ij}}{k_i}. \tag{3.1}$$

By definition, the normal random walker hops with equal probability from a node to one of its nearest neighbours in the network. In addition, from Eq. (2.6), the stationary distribution is $P_i^{\infty} = \frac{k_i}{\sum_{l=1}^{N} k_l}$. Normal random walks have been extensively studied in different contexts with applications in diverse types of networks; in particular, lattices [7, 16], general graphs [17, 59], complex networks [22, 60–62], fractal and recursive structures [63, 64], among others [27].

3.2 *Preferential navigation: biased random walk*

In the preferential navigation, a random walker hops with transition probabilities $\pi_{i\to j}$ that depend on the quantity $q_i > 0$ assigned to each node i of the network. The value q_i can represent a topological feature of the respective node (e.g. the degree, the betweenness centrality, the eigenvector centrality, the clustering coefficient, among other measures [13]) or a value, independent of the network structure, that quantifies an existing resource at each node. We define preferential random walks with local information by means of the weights $\Omega_{ij} = (q_i q_j)^{\beta} A_{ij}$, where the exponent β is a real parameter. Then, from Eq. (2.2), we have

$$\pi_{i\to j} = \frac{A_{ij} q_j^{\beta}}{\sum_{l=1}^{N} A_{il} q_l^{\beta}}. \tag{3.2}$$

In Eq. (3.2), $\beta > 0$ describes the tendency to hop to neighbour nodes with large values of q, whereas for $\beta < 0$ this behaviour is inverted and the walker tends to hop to nodes with lower values of q. On the other hand, for $\beta = 0$ the normal random walk is recovered. By means of Eq. (2.6), the stationary distribution for the preferential random walk is

$$P_i^{\infty} = \frac{\sum_{l=1}^{N} (q_i q_l)^{\beta} A_{il}}{\sum_{l,m=1}^{N} (q_l q_m)^{\beta} A_{lm}}. \tag{3.3}$$

As we will see in the next part, the general preferential random walker defined by Eq. (3.2) determines different types of local random walks depending on the selection of the quantities q_i.

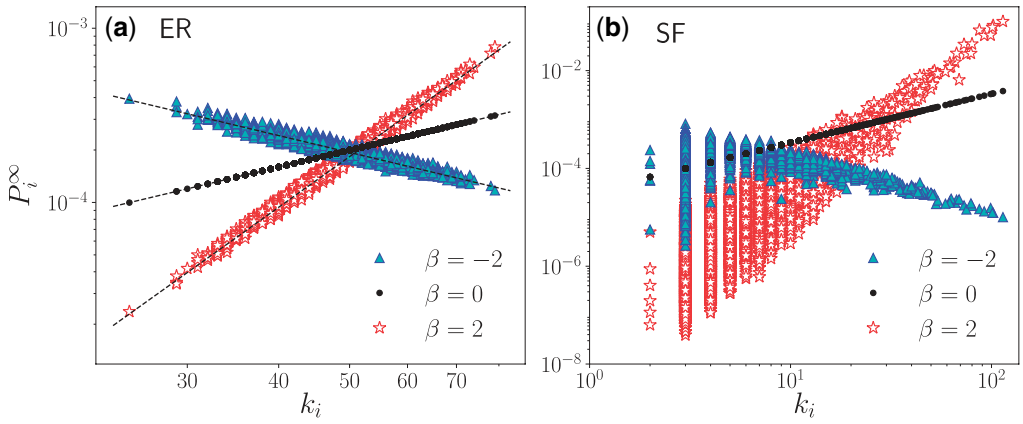

FIG. 2. Stationary distribution P_i^∞ as a function of k_i for degree biased random walks. The values are obtained by direct evaluation of Eq. (3.4). We use three values of the parameter β and we study two types of networks with $N = 5000$ nodes. (a) An ER network with an average degree $\langle k \rangle = 50$; the dashed lines represent the results obtained by the mean field approximation. (b) A SF network with $\langle k \rangle = 6$.

3.3 *Degree biased random walks*

This type of random walk is a particular case of the preferential navigation with $q_i = k_i$ in Eq. (3.2). The resulting model is known as degree biased random walk [20, 65]. For this particular case, the stationary distribution P_i^∞ takes the form

$$P_i^\infty = \frac{\sum_{l=1}^{N} (k_i k_l)^\beta A_{il}}{\sum_{l,m=1}^{N} (k_l k_m)^\beta A_{lm}}. \tag{3.4}$$

Degree biased random walks have been studied extensively in the literature in different contexts as varied as routing processes [65], chemical reactions [66], extreme events [67, 68], among others [20, 69, 70]. Additionally, mean field approximations have been explored for diverse cases [20, 66, 71]. For example, in networks with no degree correlations is valid the approximation $P_i^\infty \approx \frac{k_i^{\beta+1}}{\sum_{l=1}^{N} k_l^{\beta+1}}$. In Fig. 2, we present the values of the stationary distribution P_i^∞ for degree biased random walks on an Erdős–Rényi network (ER) and a scale-free network (SF) of the Barabási–Albert type, in which each node has a degree that follows asymptotically a power-law distribution $p(k) \sim k^{-\gamma}$ [13, 14]. We calculate the stationary distribution by direct evaluation of Eq. (3.4), and we depict P_i^∞ as a function of the degree k_i. The results reveal that in the ER network the mean-field approximation is valid whereas in a SF network, this is only valid for nodes with high degrees [20].

3.4 *Maximal entropy random walks*

Maximum entropy random walks (MERW) are a particular model derived from Eq. (3.2) for which the random walker uses information of the neighbouring nodes. In this case, the transition probability is defined in terms of the components of the eigenvector centrality ξ_i of the node i. The value ξ_i is determined by the ith component of the normalized eigenvector $\vec{\xi}$ of the adjacency matrix $\mathbf{A}$ that satisfies

$\mathbf{A}\vec{\xi} = \chi\vec{\xi}$, where χ is the maximum eigenvalue of $\mathbf{A}$. In the study of topological features of networks, the components ξ_i of the eigenvector centrality quantify the global influence of the node i in the whole structure [13].

In this way, MERW are defined in the formalism of weighted networks with the choice of weights $\Omega_{ij} = \xi_i \xi_j A_{ij}$. Then, the value of the strength S_i is

$$S_i = \sum_{l=1}^{N} \Omega_{il} = \sum_{l=1}^{N} \xi_i \xi_l A_{il} = \xi_i \sum_{l=1}^{N} A_{il}\xi_l = \chi \xi_i^2, \tag{3.5}$$

where the last result is a consequence of the relation $\sum_{l=1}^{N} A_{il}\xi_l = \chi\xi_i$ that satisfy the components of the eigenvector centrality. In this way, by using Eq. (2.2), the transition rule $\pi_{i\to j}$ is given by

$$\pi_{i\to j} = A_{ij}\frac{\xi_i\xi_j}{\chi\xi_i^2} = A_{ij}\frac{\xi_j}{\chi\xi_i}, \tag{3.6}$$

a relation that defines a maximal entropy random walk [72]. Additionally, by using the Eq. (2.6), the stationary distribution of the maximal entropy random walk is

$$P_i^{\infty} = \frac{\chi\xi_i^2}{\sum_{l=1}^{N}\chi\xi_l^2} = \xi_i^2. \tag{3.7}$$

It is worth to mention that, the MERW defined by the transition probabilities in Eq. (3.6) maximizes the entropy rate production h of the process given by [72]

$$h = -\sum_{i=1}^{N} P_i^{\infty} \sum_{j=1}^{N} \pi_{i\to j} \log \pi_{i\to j}. \tag{3.8}$$

Combining this expression with Eqs. (3.6) and (3.7), $h = \log\chi$ [72]. In this case, the trajectories that follow the random walker are maximally random [72, 73]. Diverse variations of the MERW and applications of this process have been explored in Refs. [73–76].

3.5 *Random walks for image segmentation*

An important application of random walks on networks emerges in the context of the processing and segmentation of digital images [77]. In this case, the statistical description of the diffusive transport from seed regions to specific pixels allows to detect and differentiate objects and structures in a digital image [77]. The network is a square lattice where each node represents a pixel and the normalized intensity $\mathscr{I}_i$ of i is a quantity associated to the norm of the vector $\vec{p}_i$ that contains the values RGB (red, green and blue) of the respective pixel, $0 \leq \mathscr{I}_i \leq 1$. In terms of a matrix of weights Ω, a local random walker is defined by [77]

$$\Omega_{ij} = \exp\left[-(\mathscr{I}_i - \mathscr{I}_j)^2/\sigma^2\right] A_{ij}. \tag{3.9}$$

Here, the real parameter σ satisfies $\sigma > 0$ and the values A_{ij} give the elements of the adjacency matrix of a square lattice associated to the pixel positions and interactions between nearest neighbours. The resulting

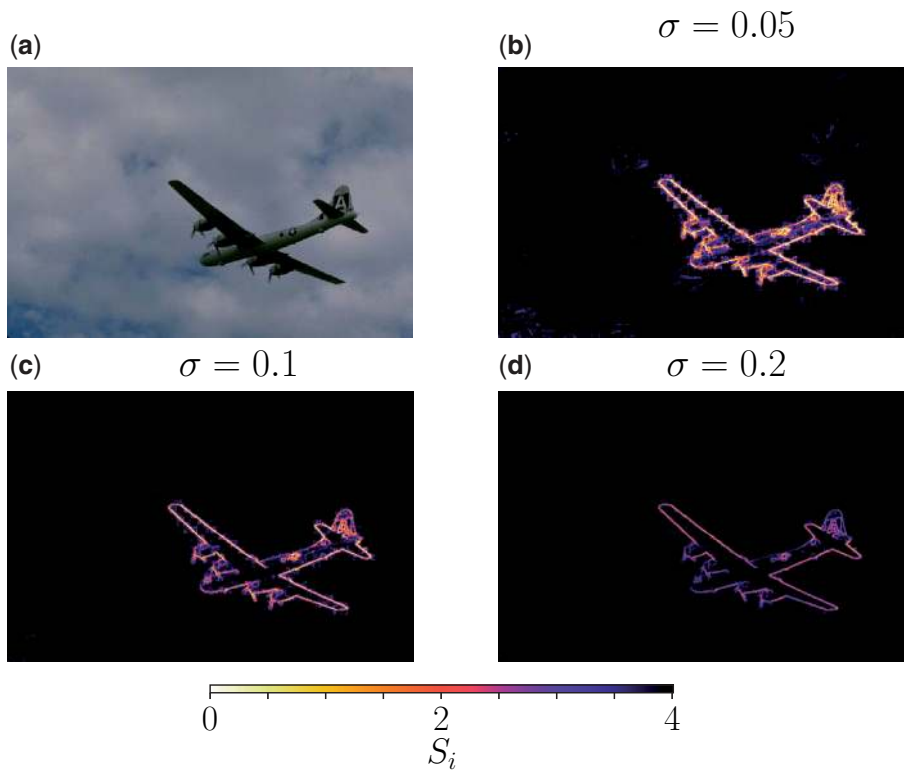

FIG. 3. Strength S_i for random walks in the context of image segmentation. The values are obtained evaluating the sum $S_i = \sum_{l=1}^{N} \Omega_{il}$ with the weights given by Eq. (3.9). In (a), we present the original image (#3096 from the Berkeley segmentation database BSD300 [86]). In (b)–(d), we present the results obtained for different values of the parameter σ; the colourbar denotes the scale of values for S_i. Regions with $S_i = 4$ present little variations in the intensity of a pixel in relation with its nearest neighbours, in these regions the random walker behaves as a normal random walker.

random walker follows a dynamics given by Eq. (2.2) to visit the pixels; this transition probability gives high probability to the pass to pixels with the same intensity and σ determines the interaction between the pixels establishing a characteristic scale for the differences of intensity in the model controlling the capacity to hop to sites with a different colour. In Fig. 3, we plot the strength S_i for each pixel; this quantity is proportional to the stationary probability distribution for a random walker in a digital image determined by the weights given by Eq. (3.9). It is observed how with this random walk, S_i takes high values in regions with uniform colour and low values in the boundaries of the object. In this way, the random walker propagates uniformly in zones with the same colour and with low probability passes through the boundary of the object. This property makes this type of weights good candidates for image segmentation algorithms.

In addition to the local dynamics mentioned before, it is worth mentioning that there are different variations of these models. This is the case of the topological biased random walks for which $\Omega_{ij} = e^{\beta y_{ij}} A_{ij}$ [78], where the quantity y_{ij} describes the properties of the edge that connects i with j. A similar idea is explored for image segmentation in Ref. [79], showing the vast applicability of random walks in different scenarios.

4. Non-local random walk models

Non-local random walks on networks are motivated by the possibility of hopping from one node to sites on the network beyond the neighbouring nodes in cases where the total structure of the network is available. Random walks with long-range displacements have shown an unprecedented applicability in the context of web searching. The PageRank introduced to classify pages on the Web [80] and variations of this non-local model have been explored to rank the importance of nodes in a broad range of systems. In this section, we present different non-local strategies on networks in terms of a matrix of weights that includes global information of the network to define the dynamical process. As particular examples of this case we have the Lévy flights on networks introduced for the first time in [30], the fractional diffusion on networks introduced for the first time in [39], the movement of agents visiting specific locations in a city [28], different dynamics in the context of the random multi-hopper model [37] and the path Laplacian of a graph [81–85]. In the following, we will discuss in detail some of the non-local random walks and make a comparison between them with the corresponding local random walks.

4.1 *Lévy-like dynamics on networks*

The term Lévy flights refers to a random walk with displacements of random lengths l given by a probability distribution $\mathscr{K}(l)$ that asymptotically is described by an inverse power-law relation [87, 88]. For Lévy flights in the n-dimensional space $\mathbb{R}^n$, $\mathscr{K}(0) = 0$ and $\mathscr{K}(l) \sim \frac{1}{l^{n+2\gamma}}$ if $l \neq 0$ and $0 < \gamma < 1$. With this definition, the variance of the displacements diverges; this characteristic differentiates Lévy flights from Brownian motion, for which the variance is finite [7]. In Fig. 4, we present Monte Carlo simulations for Brownian motions and Lévy flights in a continuous two-dimensional region. Lévy flights have a fractal behaviour consisting of trajectories that alternate between groups described by local movements (similar to the observed in the Brownian motion) interrupted by long-range jumps; this structure is repeated at all levels. In this way, Lévy flights combine local movements that appear with high probability, with long-range displacements that emerge with low but non-null probability. These characteristics are illustrated in Fig. 4(b). Lévy flights constitute an active area of research in different complex systems. For example, Lévy flights are encountered in the modelling of animal dynamics and foraging [6, 89–92], human mobility [93–95], among many others [87, 88, 96].

In the context of networks, Lévy-like dynamics were introduced for the first time in Ref. [30]. In this case, the transitions are defined in terms of the geodesic distance d_{ij}, given by the number of links in the shortest path connecting the nodes i and j. All the information about the distances between nodes is contained in the distance matrix $\mathbf{D}$ with elements d_{ij} for $i, j = 1, 2, \ldots, N$. The distance matrix $\mathbf{D}$ have more information about the structure of the network than the adjacency matrix $\mathbf{A}$, and $\mathbf{D}$ can be calculated efficiently from $\mathbf{A}$ using several algorithms [13]. In Fig. 5, we depict the relative frequency of distances in the entries of the matrix $\mathbf{D}$ for large-world networks (square lattice and tree) and small-world networks (ER network and SF network of the Barabási–Albert type). The histograms reveal the marked difference between the distances in these two types of networks.

A Lévy like dynamics on networks can be described in terms of the weights $\Omega_{ij} = d_{ij}^{-\alpha}$ for $i \neq j$ and $\Omega_{ii} = 0$. Here, α is a real parameter in the interval $0 \leq \alpha < \infty$. For the elements of the transition matrix, we have $\pi_{i\to i} = 0$ and using Eq. (2.2) for $i \neq j$, we obtained [30]

$$\pi_{i\to j} = \frac{d_{ij}^{-\alpha}}{\sum_{l\neq i} d_{il}^{-\alpha}}. \tag{4.1}$$

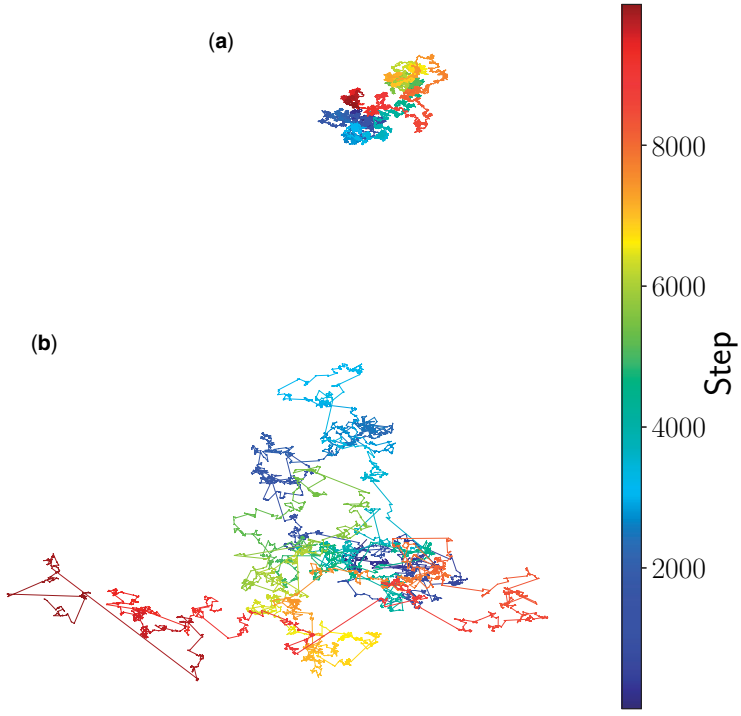

FIG. 4. Monte Carlo simulations of two different types of random walks on a continuous two-dimensional region. (a) Brownian motion. (b) Lévy flights. We depict 10^4 steps for each realization. The colourbar codifies the discrete time.

In the following, we refer to this model as '*Lévy flights*' or '*Lévy random walk*' on networks. In this case, the dynamics allows long-range transitions on the network. For a finite non-null value of α the transitions to the nearest neighbours appear with high probability, but hops beyond these nodes are allowed generalizing the movement observed in the normal random walker in Eq. (3.1). In the limit $\alpha \to \infty$ we have $\lim_{\alpha\to\infty} d_{ij}^{-\alpha} = A_{ij}$, then $\pi_{i\to j} = \frac{A_{ij}}{k_i}$ and the normal random walk is recovered. Another interesting limiting case is obtained when $\alpha \to 0$: here, $\lim_{\alpha\to 0} d_{ij}^{-\alpha} = 1$ if $i \neq j$ and then we have an equal probability to reach any node of the network [30].

Thus, for Lévy flights, we have $\Omega_{ij} = d_{ij}^{-\alpha}$ for $i \neq j$. For this particular model, we denote the strength $S_i = \sum_{l=1}^{N} \Omega_{il}$ as $D_i^{(\alpha)} = \sum_{l\neq i} d_{il}^{-\alpha}$ and by using the Eq. (2.6), we obtain for the stationary distribution

$$P_i^{\infty} = \frac{D_i^{(\alpha)}}{\sum_{l=1}^{N} D_l^{(\alpha)}} = \frac{\sum_{l\neq i} d_{il}^{-\alpha}}{\sum_{l\neq m}\sum_{m} d_{lm}^{-\alpha}}. \tag{4.2}$$

This result establishes that P_i^{∞} is proportional to the quantity $D_i^{(\alpha)}$. In addition, the value $D_i^{(\alpha)}$, can be expressed as [30]

$$D_i^{(\alpha)} = \sum_{l=1}^{N-1} \frac{1}{l^{\alpha}} n_i^{(l)} = k_i + \frac{n_i^{(2)}}{2^{\alpha}} + \frac{n_i^{(3)}}{3^{\alpha}} + \ldots, \tag{4.3}$$

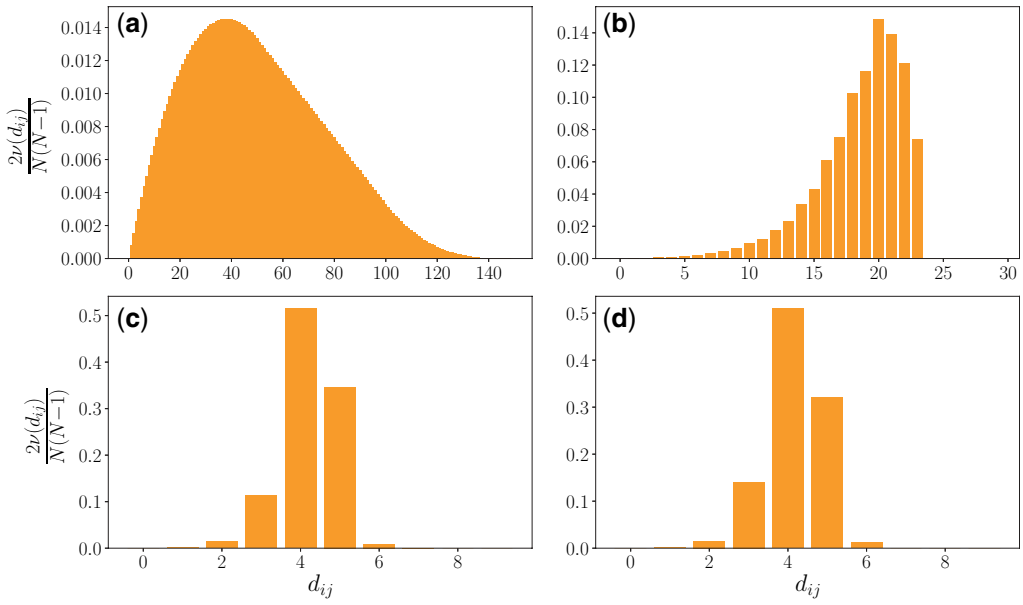

FIG. 5. Frequencies $\nu(d_{ij})$ of the non-null distances d_{ij} in the entries of the distance matrix $\mathbf{D}$. We analyse networks with $N = 5000$. (a) Square lattice with dimensions 50×100. (b) Tree. (c) ER network with probability of connection $p = \frac{\log N}{N}$. (d) SF network of the Barabási–Albert type. The results are expressed as a fraction of the value $N(N-1)/2$ that gives the total number of different non-null entries in the distance matrix $\mathbf{D}$. In these histograms is clear the difference between the large-world networks (a) and (b), and the small-world networks (c) and (d).

where $n_i^{(l)}$ is the number of nodes at a distance l of the node i; in particular, $n_i^{(1)} = k_i$. In this way, by means of the expression in Eq. (4.3) we observe that $D_i^{(\alpha)}$ is a generalization of the degree k_i that combines all the information about the structure of the network. This long-range degree emerges from the study of Lévy flights on networks and was introduced in Ref. [30].

In Fig. 6, we depict the stationary distribution obtained from the analytical result in Eq. (4.2) for an ER network and a SF network. Also notice that, compared to the normal random walk, Lévy flights represent a more uniform dynamics in the sense that the probability of visiting sites with many connections decreases and for sites with a lower degree, this probability increases. Being able to easily reach any node on the network can offer an advantage if the goal is to explore the entire structure.

Different aspects of Lévy flights and their capacity to explore networks have been studied in Refs. [32–35], as well as in the context of multiplex networks [31]. A general approach to study the random walker in Eq. (4.1), as well as other models with different functions of the distances in a network are analysed in detail by Estrada *et al.* in Ref. [37]. In that paper, we introduced the exponential random walk that in terms of our matrix of weights formalism is defined by $\Omega_{ij} = e^{-sd_{ij}}$ for $i \neq j$ and $s > 0$. By following a similar approach to the one presented here in Eqs. (4.2)–(4.3), it can be obtained analytical expressions for the stationary probability distribution of the exponential case.

4.2 *Gravity law, spatial networks and human mobility*

In diverse situations networks are embedded in a metric space, then, spatial locations are assigned to each node. This is the case of spatial networks that describe several real systems like airports and transportation

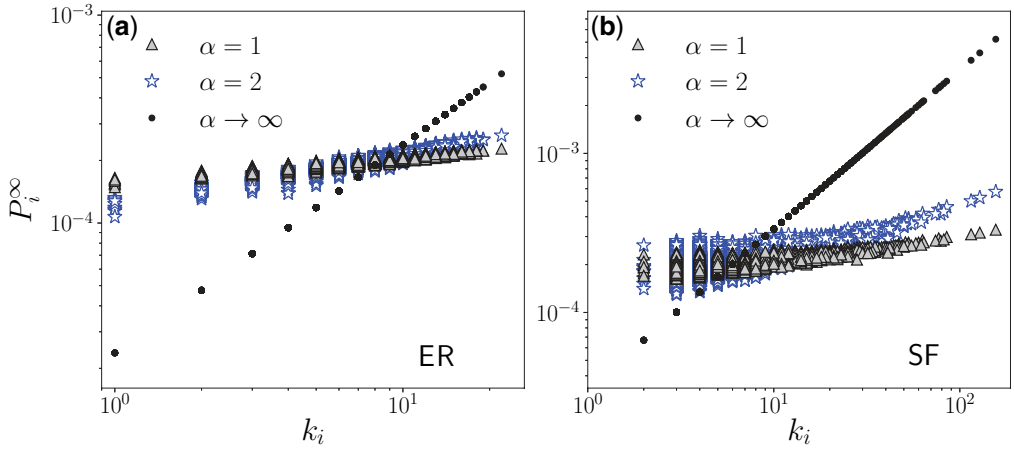

FIG. 6. Stationary distribution P_i^∞ in terms of the degree k_i for Lévy flights on networks with $N = 5000$. The models with $\alpha = 1$ and $\alpha = 2$ use long-range displacements in the network. The result for the normal walker (limit $\alpha \to \infty$) is also depicted.

networks, infrastructure networks and many others [32, 97]. In particular, an important instance where spatial networks become relevant are the recent studies of human mobility in cities [98–101].

It has been suggested that migration and human movements are well described in terms of a 'Gravity Law' that models the number of trips from a location i to a location j as $g_{ij} = C\, p_i p_j / l_{ij}^\alpha$. Here p_i and p_j denote the population of the respective locations, l_{ij} is the geometric (metric) distance between the nodes i, j, C is a constant and $\alpha > 0$ is a free parameter [98–100]. This type of model suggests a similar algorithm for a random walker on networks described by the weights

$$\Omega_{ij} = \frac{q_i q_j}{d_{ij}^\alpha} \tag{4.4}$$

for $i \neq j$. Here, the value q_i is a quantity associated to the node i in the network and d_{ij} is the geodesic distance in the network. The general formalism in terms of weighted networks also applies to the model presented in Eq. (4.4), but with geometric (metric) distances l_{ij}. In this model, the structure of the network is absent but mathematically can be equivalent to a weighted network with weights given by Eq. (4.4).

In the gravity law model, the resulting random walker contains characteristics of the biased random walks determined by Eq. (3.2) and the Lévy flights on networks with transition probabilities given by Eq. (4.1). Additionally, there are other models, beside the gravity law, like the radiation model described in [102], that contain more general functions of the distance $f(d_{ij})$ [98–100].

As an example of random walks that take place in a continuous space but can be modelled with the formalism of random walks defined in terms of a matrix of weights, in Ref. [28], we introduced a model of a walker, that randomly visit locations in a two-dimensional spatial region, that represents the human mobility between sites in a city. In this case, N points are located in a two-dimensional region and the integer numbers $i = 1, 2, \ldots, N$ label each location. In addition, the coordinates of the locations are known, and we denote as l_{ij} the distance between the places i and j. The distance $l_{ij} = l_{ji} \geq 0$ can be calculated by different metrics; for example, in some applications could be appropriated to use an Euclidean metric, whereas, in other contexts, a Manhattan distance could be more useful. In order to define a discrete time random walker that at each step visits one of the locations, the transition probability

$\pi_{i\to j}^{(\alpha)}(R)$ to hop from site i to site j is given by [28]

$$\pi_{i\to j}^{(\alpha)}(R) = \frac{\Omega_{ij}^{(\alpha)}(R)}{\sum_{m=1}^{N}\Omega_{im}^{(\alpha)}(R)}, \tag{4.5}$$

where the weights $\Omega_{ij}^{(\alpha)}(R)$ are defined by the relation [28]

$$\Omega_{ij}^{(\alpha)}(R) = \begin{cases} 1 & \text{for} \quad 0 \le l_{ij} \le R, \\ \left(R/l_{ij}\right)^{\alpha} & \text{for} \quad R < l_{ij}. \end{cases} \tag{4.6}$$

Here, α and R are positive real parameters. The radius R determines a neighbourhood around which the random walker can go from the initial site to any of the locations in this region with equal probability; this transition is independent of the distance between the respective sites. That is, if there are S sites inside a circle of radius R, the probability of going to any of these sites is constant. Additionally, for places beyond the local neighbourhood, for distances greater than R, the transition probability decays as an inverse power law of the distance and is proportional to $l_{ij}^{-\alpha}$ [28]. In this way, the parameter R defines a characteristic length of the local neighbourhood and α controls the capacity of the walker to hop with long-range displacements. In particular, in the limit $\alpha \to \infty$ the dynamics becomes local, whereas the case $\alpha \to 0$ gives the possibility to go from one location to any different one with the same probability. In this limit, we have $\pi_{i\to j}^{(0)}(R) = N^{-1}$. This model is then a combination of a rank model [103–105] for shorter distances and a gravity-like model for larger ones [98]. It is important to mention that in the movement defined by the weights in Eq. (4.6), we choose $\Omega_{ii}^{(\alpha)}(R) \neq 0$; in this way the walker can stay in the node i with non-null probability. All the results presented here are also valid for this case, whenever the value of R is such that the random walker can reach any of the N sites used in the definition of the transition matrix.

In Fig. 7(a), we illustrate the model for the random walk introduced in Eq. (4.5). In Fig. 7(b), we present Monte Carlo simulations of the random walker described by Eqs. (4.5)–(4.6). We generate N random locations (points) on a continuous region $[0,1] \times [0,1]$ in $\mathbb{R}^2$ and, for different values of the exponent α, we depict the trajectories described by the walkers. In the case of $\alpha \to \infty$, it is observed that the dynamics is local and only allows transitions to sites in a neighbourhood determined by a radius $R = 0.17$ around each location. In this case, all the possible trajectories in the limit $t \to \infty$ form a random geometric graph [106, 107]; we can identify features of this structure in our simulation. On the other hand, finite values of α model spatial long-range displacements such as the results illustrated in Fig. 7(b) for the case $\alpha = 4$. We observe how the introduction of the long-range activity improves the capacity of the random walker to visit and explore more locations in comparison with the local dynamics defined by the limit $\alpha \to \infty$ [28].

4.3 *The Fractional Graph Laplacian*

The fractional transport on networks is defined in terms of a power of the Laplacian matrix $\mathbf{L}$ with elements given by $L_{ij} = \delta_{ij}k_i - A_{ij}$, where δ_{ij} denotes the Kronecker delta; in particular, $L_{ii} = k_i$. That is, the Laplacian matrix is defined as a diagonal matrix, that has the degrees of the nodes as diagonal elements, minus the adjacency matrix. The graph Laplacian matrix is introduced in graph theory and in the modeling of diffusion processes on networks [14, 18, 108–114]. In addition, the matrix $\mathbf{L}$ is related with the discrete form of the Laplacian operator $(-\nabla^2)$ that appears in the diffusion equation in the continuum [13, 113, 114].

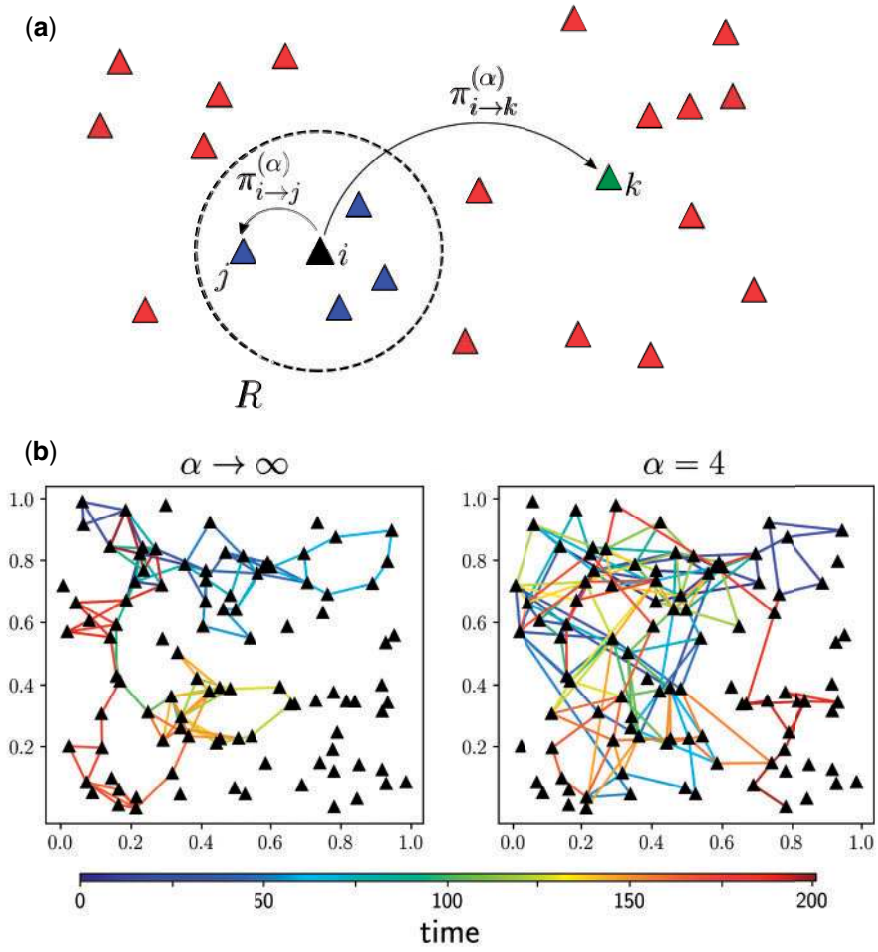

FIG. 7. A schematic illustration of the random walk defined in Eq. (4.5). In (a) we depict random locations on the continuous two-dimensional region (represented by triangles); the probability to go from location i to a different site is determined by two types of transition probabilities: First, to a site j inside a circular region of radius R centred in the location i, $\pi^{(\alpha)}_{i\to j}(R)$, which is a constant; and second, a transition to a site k outside the circle of radius R, $\pi^{(\alpha)}_{i\to k}(R)$ that considers long-range transitions with a power-law decay proportional to $l_{ik}^{-\alpha}$, where l_{ik} is the distance between sites i and k. In (b) we show Monte Carlo simulations of a discrete-time random walker that visits $N = 100$ specific locations in the region $[0, 1] \times [0, 1]$ in $\mathbb{R}^2$ following the random movement defined by the transition probabilities in Eq. (4.5), with $R = 0.17$. We depict the results for $\alpha \to \infty$ and $\alpha = 4$. The total number of steps is $t = 200$ and the scale in the colour bar represents the time at each step.

The Laplacian operator that appears in the diffusion equation gives rise to normal diffusion processes, associated with the normal Brownian motion [115], for instance. However, it is well known that an extension to the Fractional Calculus of the Laplacian operator leads to a fractional partial differential equation: the fractional diffusion equation in the continuum. This equation describe anomalous diffusion and long-range processes, like Lévy flights, among other anomalous processes. There is a vast literature

of fractional dynamics, see for instance the following books and review papers [87, 96, 116–119]. Thus, we have in the continuum the usual Laplacian and its counterpart, the fractional Laplacian. On the other hand, in a graph (network) we do have a normal Graph Laplacian, as described above. However, what has been lacking, until recently, was a Fractional Graph Laplacian that acts on a network. In 2014, Riascos and Mateos [39] introduced, for the first time, a *Fractional Graph Laplacian* on a general network $\mathbf{L}^{\gamma}$, where the real number γ is the fractional index defined in the interval $0 < \gamma < 1$.

Since the Laplacian matrix $\mathbf{L}$ is a symmetric matrix, by using the Gram–Schmidt orthonormalization of the eigenvectors of $\mathbf{L}$, we obtain a set of eigenvectors $\{|\Psi_j\rangle\}_{j=1}^{N}$ that satisfy the eigenvalue equation $\mathbf{L}\,|\Psi_j\rangle = \mu_j\,|\Psi_j\rangle$ for $j = 1,\ldots,N$ and $\langle\Psi_i|\Psi_j\rangle = \delta_{ij}$, where μ_j are the eigenvalues, which are real and nonnegative. Here, we are using the notation of Dirac brackets, as is usual in the literature of physics. For connected networks, the smallest eigenvalue is $\mu_1 = 0$ and $\mu_m > 0$ for $m = 2,\ldots,N$ [15]. We define the matrix $\mathbf{Q}$ with elements $Q_{ij} = \langle i|\Psi_j\rangle$ and the diagonal matrix $\Lambda = \mathrm{diag}(0,\mu_2,\ldots,\mu_N)$. These matrices satisfy $\mathbf{L}\,\mathbf{Q} = \mathbf{Q}\,\Lambda$, therefore $\mathbf{L} = \mathbf{Q}\Lambda\mathbf{Q}^{\dagger}$, where $\mathbf{Q}^{\dagger}$ denotes the conjugate transpose of $\mathbf{Q}$. Therefore, following well-known results of linear algebra (see [120]), Riascos and Mateos define in [39] the fractional graph Laplacian as:

$$\mathbf{L}^{\gamma} = \mathbf{Q}\Lambda^{\gamma}\mathbf{Q}^{\dagger} = \sum_{m=2}^{N} \mu_m^{\gamma}\,|\Psi_m\rangle\,\langle\Psi_m|\,, \tag{4.7}$$

where $\Lambda^{\gamma} = \mathrm{diag}(0,\mu_2^{\gamma},\ldots,\mu_N^{\gamma})$. It is worth noticing that the diagonal elements of the fractional graph Laplacian defined in Eq. (4.7) introduce a generalization of the degree $k_i = (\mathbf{L})_{ii}$ to the fractional case. In this way, the fractional degree $k_i^{(\gamma)}$ of the node i is given by [39]

$$k_i^{(\gamma)} \equiv (\mathbf{L}^{\gamma})_{ii} = \sum_{m=2}^{N} \mu_m^{\gamma}\langle i\,|\Psi_m\rangle\,\langle\Psi_m|\,i\rangle. \tag{4.8}$$

The fractional random walk is the random walk associated with the fractional diffusion in networks. Here, we generalize the result in [39] to the case of weighted networks. In the formalism of weighted networks is defined by the elements $\Omega_{ii} = 0$ and, for $i \neq j$

$$\Omega_{ij} = -(\mathbf{L}^{\gamma})_{ij} \tag{4.9}$$

with $0 < \gamma \leq 1$. On the other hand, the elements of the Laplacian matrix satisfy $k_i = -\sum_{l\neq i} L_{il}$ and, in the fractional case we have $k_i^{(\gamma)} = -\sum_{l\neq i}(\mathbf{L}^{\gamma})_{il}$. As a result, the strength of the node i is given by

$$S_i = \sum_{l=1}^{N} \Omega_{il} = -\sum_{l\neq i}(\mathbf{L}^{\gamma})_{il} = k_i^{(\gamma)}, \tag{4.10}$$

then, by using Eq. (2.2), the transition probability $\pi_{i\to j}$ is given by

$$\pi_{i\to j} = \delta_{ij} - \frac{(\mathbf{L}^{\gamma})_{ij}}{k_i^{(\gamma)}}. \tag{4.11}$$

In the limit $\gamma \to 1$, the normal random walk is recovered. In addition, by using the Eq. (2.6), the stationary distribution is

$$P_i^{\infty} = \frac{k_i^{(\gamma)}}{\sum_{l=1}^{N} k_l^{(\gamma)}}. \tag{4.12}$$

This is a generalization of the result $P_i^{\infty} \propto k_i$ for normal random walks discussed before and recovered from Eq. (4.12) when $\gamma = 1$.

The fractional random walk is the process associated with the fractional diffusion on networks and the transition probabilities in Eq. (4.11) define a model with long-range displacements on the network [39]. The case of infinite n-dimensional lattices with periodic boundary conditions has been addressed in different contexts [45–47, 121, 122]. For this type of periodic structures, the following analytical relation is obtained [46]. For a thorough description of the Fractional dynamics on networks and lattices, see the recent book [48].

$$\pi_{i\to j} \sim d_{ij}^{-n-2\gamma} \qquad \text{for} \quad d_{ij} \gg 1. \tag{4.13}$$

The result in Eq. (4.13) establishes a connection between Lévy flights on networks [30] and the fractional dynamics defined by Eq. (4.11). That is, it can be derived from the non-local general formalism of the Fractional Graph Laplacian.

Let us now discuss a revealing result of the Fractional Graph Laplacian formalism for the particular case of regular networks. There is an important set of networks, called regular networks, where the degree of each node is the same, that is, the degree k is constant. Examples of regular networks are lattices in any dimension, triangular and hexagonal networks, regular trees and many others.

In a regular network with constant degree k, the fractional graph Laplacian can be expressed as [40]

$$(\mathbf{L}^{\gamma})_{ij} = \sum_{m=0}^{\infty} \binom{\gamma}{m} (-1)^m k^{\gamma-m} (\mathbf{A}^m)_{ij}, \tag{4.14}$$

where $\binom{x}{y} \equiv \frac{\Gamma(x+1)}{\Gamma(y+1)\Gamma(x-y+1)}$ and $\Gamma(x)$ denotes the Gamma function [123]. The result in Eq. (4.14) gives an exact expression of the fractional graph Laplacian as a sum of coefficients and inverse powers of the degree, and integer powers of the adjacency matrix $\mathbf{A}^m$ for $m = 1, 2, \ldots$. The matrix element $(\mathbf{A}^m)_{ij}$ is the number of all the possible trajectories connecting the nodes i, j with m links [124]. Therefore, the Fractional Graph Laplacian can be written as a sum of trajectories in the network where each trajectory has a coefficient that gives a weight in the sum. Notice that the longer the trajectory the smaller the coefficient that measures the contribution in the sum. In this way, the fractional dynamics, defined by the transition matrix with elements $\pi_{i\to j}$ in Eq. (4.11), incorporates global (non-local) information about all the possible trajectories connecting the nodes i and j. This result was obtained for regular networks in [40].

Here, it is worth mentioning that $\mathbf{L}^{\gamma}$ for $0 < \gamma < 1$ describes the non-local structure of a network, and only the normalized version in Eq. (4.11) defines entries that can be interpreted as transition probabilities to jump or move on the network. This process is associated with the fractional diffusion and Lévy flights on networks [40, 48]. In continuous-time, fractional diffusive transport is defined by the matrix

$$\mathscr{L}^{(\gamma)} = \mathbb{I} - \Pi^{(\gamma)}, \tag{4.15}$$

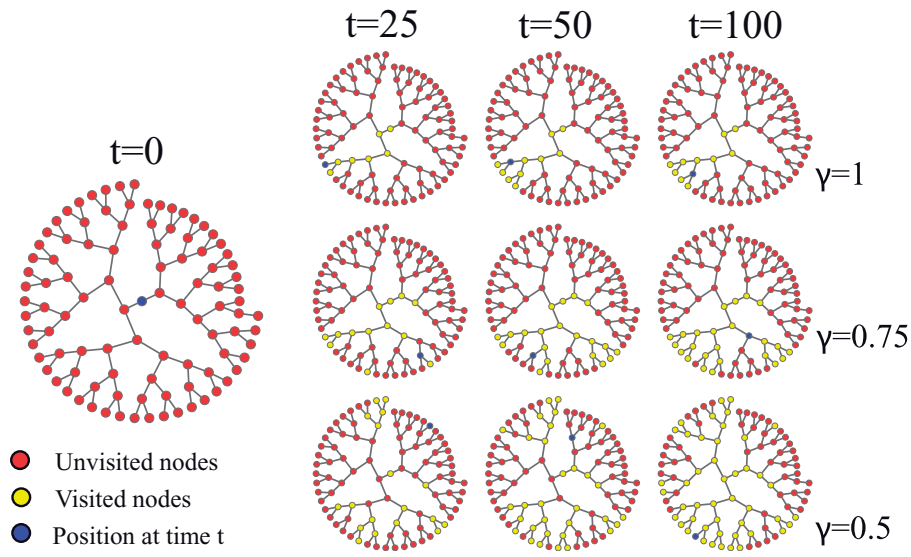

FIG. 8. Monte Carlo simulation of a discrete-time fractional random walker on a tree with transition probabilities given by Eq. (4.11). The movement starts at $t = 0$ from an arbitrary node. We show three discrete times $t = 25, 50, 100$ for three values of the parameter $\gamma = 1, 0.75, 0.5$. The case $\gamma = 1$ corresponds to a normal random walker whereas the cases with $\gamma = 0.75, 0.5$ correspond to a fractional random walk leading to anomalous transport. We represent with different colours the unvisited nodes, visited nodes and the position of the random walker at time t.

where $\mathbb{I}$ is the $N \times N$ identity matrix and $\Pi^{(\gamma)}$ is defined by the elements $\pi_{i\to j}$ in Eq. (4.11); see Ref. [39] for a detailed discussion. In general networks, the dynamics defined by $\mathbf{L}^{\gamma}$ cannot be interpreted as hops between nodes or diffusive transport. These types of interpretations can lead to counterintuitive conclusions, showing that the normalization in Eq. (4.15) is required in a proper analysis of continuous-time diffusive transport on networks.

In order to illustrate the effect of the fractional dynamics of a random walker on a network, in Fig. 8, we present Monte Carlo simulations of discrete-time random walks on a tree. The discrete time t denotes the number of steps of the random walker as it moves from one node to the next node on the network. Given the topology of the network, we calculate the adjacency matrix and the corresponding Laplacian matrix $\mathbf{L}$ of the network. Then we obtain its eigenvalues and eigenvectors that allow us in turn to get the fractional graph Laplacian $\mathbf{L}^{\gamma}$. Finally, using Eq. (4.11), we determine the transition probabilities for different values of the parameter γ. The movement starts at $t = 0$ from an arbitrary node. We show three discrete times $t = 25, 50, 100$ for three values of the parameter $\gamma = 1, 0.75, 0.5$. Here, we depict one representative realization of a random walker as it hops from one node to another randomly. The case $\gamma = 1$ corresponds to normal random walk leading to normal diffusion. In this case, the random walker can move only locally to nearest neighbours and, as can be seen in the figure, the walker revisits frequently the same nodes and therefore the exploration of the network is redundant and slow. The cases with $\gamma = 0.75$ and 0.5 correspond to a fractional random walk leading to anomalous diffusion. In this case, the random walker can move in a long-range fashion from one node to another arbitrarily distant node. This allows us to explore more efficiently the network since the walker does not tend to revisit the same nodes; on the contrary, it tends to explore new distant regions each time. All this can be seen in the figure for different times, and allow us to make a comparison between a random walker using regular

dynamics and a fractional dynamics [40]. A detailed analysis of the fractional graph Laplacian and its relation with long-range dynamics on networks and applications is presented in Refs. [39, 40, 43–47, 122].

The introduction of the fractional random walks is motivated by the search of an equivalent on networks of the fractional diffusion and its relation with Lévy flights. Recently, other types of functions of matrices with local information have shown interesting properties associated with long-range dynamics and the global structure of networks; this is the case of the communicability [110, 125] and the random walk accessibility introduced in Ref. [126]. Particular functions of matrices can be used to define different types of long-range random walks and characterized with the formalism reviewed in this work.

As a generalization of Eq. (4.11), other functions of the Laplacian $g(\mathbf{L})$ can be applied to define random walk strategies on networks. In order that the functions $g(x)$ properly define random walk models, they should satisfy the following conditions [56]

- **Condition I:** The matrix $g(\mathbf{L})$ must be positive semidefinite, that is, the eigenvalues of $g(\mathbf{L})$ are restricted to be positive or zero. In this way, the property of the Laplacian eigenvalues $\mu_i \geq 0$ for $i = 2, \ldots, N$ is preserved by the function $g(x)$.
- **Condition II:** The elements of the matrix $g(\mathbf{L})$ denoted as $g_{ij}(\mathbf{L})$, for $i, j = 1, 2, \ldots, N$, should satisfy

$$\sum_{j=1}^{N} g_{ij}(\mathbf{L}) = 0. \tag{4.16}$$

  Therefore, the function $g(x)$ maintains the property $\sum_{j=1}^{N} L_{ij} = 0$ associated with the elements of the Laplacian matrix.
- **Condition III:** All the non-diagonal elements of $g(\mathbf{L})$ must satisfy

$$g_{ij}(\mathbf{L}) \leq 0. \tag{4.17}$$

For this type of functions, transition probabilities are defined by the relation

$$\pi_{i\to j} = \delta_{ij} - \frac{g_{ij}(\mathbf{L})}{\mathscr{K}_i}, \tag{4.18}$$

where we use the generalized degrees $\mathscr{K}_i$ defined by the diagonal elements of $g(\mathbf{L})$ that satisfy [56]

$$\mathscr{K}_i = g_{ii}(\mathbf{L}) = -\sum_{l\neq i} g_{il}(\mathbf{L}) > 0. \tag{4.19}$$

Examples of functions that satisfy the conditions I, II and III are the fractional graph Laplacian $g(\mathbf{L}) = \mathbf{L}^{\gamma}$ with $0 < \gamma < 1$, the logarithmic function $g(\mathbf{L}) = \log(\mathbb{I} + \alpha\mathbf{L})$ for $\alpha > 0$ and the function $g(\mathbf{L}) = \mathbb{I} - e^{-a\mathbf{L}}$ with $a > 0$. In all these cases, it is observed that the random walker hops with long-range displacements on the network [56].

As we commented above, functions $g(x) = x^{\gamma}$ with exponents $0 < \gamma \leq 1$ are admissible to define random walk dynamics. Powers with $\gamma > 1$ are not, since they do not fulfil Eq. (4.17).

From this observation it follows that admissible functions $g(x)$ obey (up to positive multipliers) for small arguments

$$g(x) \sim x^{\gamma}, \qquad x \to 0+, \qquad 0 < \gamma \leq 1. \tag{4.20}$$

The lowest order in the expansion of an admissible function $g(x)$ either starts with x (type (i)) that is integer $\gamma = 1$, or with x^{γ} ($0 < \gamma < 1$, type (ii)) when it is non-integer (fractional). The expansion of $g(x)$ (up to unimportant positive multipliers) for type (i) functions are of the form $g(x) = x + \tilde{g}(x) \ldots$, whereas type (ii) functions have expansions that write as $g(x) = x^{\gamma} + \tilde{g}(x) \ldots$ ($0 < \gamma < 1$). The parts $\tilde{g}(x)$ contain only powers greater than 1 in case (i), and greater than γ in case (ii), respectively. The classes (i) and (ii) are the only two classes of functions that are admissible. In view of the examples considered above, the functions $1 - e^{-x}$ and $\log(1 + \alpha x)$ are type (i) functions, whereas x^{γ} ($0 < \gamma < 1$) is of type (ii).

In Ref. [56], Michelitsch *et al.* showed that the lowest power in the expansion of $g(\mathbf{L})$ determines the dominant asymptotic transition probability for long-range steps on sufficiently large networks $N \to \infty$. In addition, functions $g(\mathbf{L}) = \mathbf{L} + \tilde{g}(\mathbf{L})$ of type (i) contain an internal length-scale defined by the local information of Laplacian $\mathbf{L}$. This type of non-locality depends on that length-scale and, by increasing the size of the network, the Laplacian functions of type (i) become quasi-local and the type (i) random walk becomes similar to a normal random walk with emerging *Brownian motions* (normal diffusion) in the limit of large networks $N \to \infty$ [48, 56].

In contrast, functions of type (ii) define a fractional type of non-locality with $g(\mathbf{L}) = \mathbf{L}^{\gamma} + \tilde{g}(\mathbf{L})$ ($0 < \gamma < 1$) which becomes asymptotically scale-free (asymptotically self-similar) in the limit of large networks $N \to \infty$. The asymptotic scale-free character wipes out, in the limit of infinite networks, any local information on $\mathbf{L}$ and in this sense is universal. In this way, type (ii) non-locality leads to the asymptotic emergence of Lévy flights (anomalous diffusion) on large networks $N \to \infty$. The type (ii) non-locality, due to its asymptotic scale-free character cannot be 'localized' as in case (i) by increasing the size N of the network. In this way, the type (ii) non-locality thus remains 'stable' when increasing the size of the network [56].

In terms of the formalism of the matrix of weights, the generalized random walk model in Eq. (4.18) can be analysed by using the weights $\Omega_{ij} = -g_{ij}(\mathbf{L})$ for $i \neq j$ and $\Omega_{ii} = 0$. In this way, as a consequence of the condition in Eq. (4.17), the weights satisfy $\Omega_{ij} \geq 0$; also, the strength of each node is given by the generalized degree $\mathscr{K}_i$ allowing us to write the stationary probability distribution of the process as

$$P_i^{\infty} = \frac{\mathscr{K}_i}{\sum_{l=1}^{N} \mathscr{K}_l}. \tag{4.21}$$

In the general case described in Eq. (4.18), the values of $g_{ij}(\mathbf{L})$ can be obtained by using the spectral methods described before for the fractional graph Laplacian (see Ref. [56] for details).

Also, it is worth mentioning that different research groups have explored non-local effects in Lévy flights and fractional transport in the context of data analysis [49, 51], the description of associative knowledge in semantic networks [127] and the introduction of Lévy Flights Graph Convolutional Networks (LFGCN) for semi-supervised learning [50]. In all these cases long-range dynamics allows both to accurately account for the network topology and to substantially improve classification performance. As a particular example of the use of the fractional graph Laplacian $\mathbf{L}^{\gamma}$, we refer to the work of Bautista *et al.* in Ref. [49], where the authors proposed the L^{γ}-PageRank, an extension of PageRank based on real powers of the Laplacian matrix. Their findings show that non-locality offers more versatility and this

TABLE 1 *Diverse types of weights Ω defining random walk models with transition probabilities $\pi_{i\to j}$ in Eq. (2.2). For all the random walk models $\Omega_{ii} = 0$. The non-diagonal elements Ω_{ij} are presented in the table with a short description of the quantities and parameters. The detailed description of each random walk is presented in Sections 3 and 4. The corresponding references are indicated in the table according to the number at the end of this article*

	Model	Weights Ω_{ij}, $i \neq j$.	Parameters	References
WEIGHTS FOR LOCAL MODELS				
1.	Normal random walk	A_{ij}		[16, 17, 21]
2.	Biased random walk	$(q_i q_j)^\beta A_{ij}$	$\beta \in \mathbb{R}$, $q_i > 0$	
3.	Degree biased random walk	$(k_i k_j)^\beta A_{ij}$	$\beta \in \mathbb{R}$	[20]
4.	Maximal entropy random walk	$\xi_i \xi_j A_{ij}$		[72, 73, 75]
5.	Random walks for image segmentation	$e^{-\frac{1}{\sigma^2}(\mathscr{I}_i - \mathscr{I}_j)^2} A_{ij}$	$\sigma > 0$	[77]
6.	Topologically biased random walk	$e^{\beta y_{ij}} A_{ij}$	$\beta \in \mathbb{R}$, $y_{ij} = y_{ji}$	[78, 79]
WEIGHTS FOR NON-LOCAL MODELS				
1.	Lévy-like dynamics	$d_{ij}^{-\alpha}$	$0 \leq \alpha < \infty$	[30, 35, 37, 129]
2.	Exponential	$e^{-s d_{ij}}$	$s > 0$	[37]
3.	Gravity Law	$q_i q_j / l_{ij}^\alpha$	$0 \leq \alpha < \infty$	[97, 130, 131]
4.	Fractional Diffusion	$-(\mathbf{L}^\gamma)_{ij}$	$0 < \gamma < 1$	[39, 40, 48]
5.	General functions of the Laplacian	$-g_{ij}(\mathbf{L})$		[48, 56]

new approach can improve the unsupervised classification in the analysis of datasets [49]. In addition, since the implementations in this case are not limited to diffusive transport, it is possible the use of $\mathbf{L}^\gamma$ with $\gamma > 1$ producing positive and negative non-diagonal entries, this particular feature reinforces the separability of clusters. The richness of such weighted networks comes from the sign of edges, allowing to consider similarities but also to emphasize dissemblance between nodes. Thus, while two nodes can only be disconnected on the initial structure, they can 'repel' themselves in non-local weighted topologies (see Ref. [49] for a discussion of $\mathbf{L}^\gamma$ with $\gamma > 1$). Finally, let us mention a very recent paper that compares the formalism of Path Laplacians, introduced by Estrada *et al.*, with our Fractional Graph Laplacian formalism as non-local operators on networks [128].

We conclude this section with a compilation of the types of random walk models represented by specific types of weighted networks. In Table 1, we summarize the matrices of weights that define the local and non-local dynamics analysed in this section. Each model is presented with the respective parameters that define the random walker and key references to works analysing these strategies.

5. Mean first passage time and global characterization

In this section, we explore the mean first passage time (MFPT) [4], that is the average number of steps needed by the random walker to reach a specific node for the first time. We also study global times that consider the MFPTs for all the nodes in order to quantify and compare the capacity of local and non-local random walks to explore different types of networks.

5.1 *MFPT*

In order to calculate the MFPT for random walks defined in terms of weighted networks, we use a similar approach to the formalism presented in Refs. [16, 21] where normal random walks are studied. We start by representing the probability $P_{ij}(t)$ in the master equation in Eq. (2.1) as

$$P_{ij}(t) = \delta_{t0}\delta_{ij} + \sum_{t'=0}^{t} P_{jj}(t-t')F_{ij}(t') \; . \tag{5.1}$$

The first term in Eq. (5.1) represents the initial condition and $F_{ij}(t)$ is the probability to start in the node i and reach the node j for the first time after t steps. By definition we have that $F_{ij}(0) = 0$. Now, by using the discrete Laplace transform $\tilde{f}(s) \equiv \sum_{t=0}^{\infty} e^{-st} f(t)$, the relation in Eq. (5.1) takes the form

$$\widetilde{F}_{ij}(s) = (\widetilde{P}_{ij}(s) - \delta_{ij})/\widetilde{P}_{jj}(s) \; . \tag{5.2}$$

By definition, using the quantity $F_{ij}(t)$, the MFPT $\langle T_{ij} \rangle$ for a random walker that starts in the node i and reach for the first time the node j is given by [16]

$$\langle T_{ij} \rangle \equiv \sum_{t=0}^{\infty} t F_{ij}(t) = -\widetilde{F}'_{ij}(0). \tag{5.3}$$

Now, by means of the moments $R_{ij}^{(n)}$ of the probability $P_{ij}(t)$ defined as

$$R_{ij}^{(n)} \equiv \sum_{t=0}^{\infty} t^n \, \{P_{ij}(t) - P_j^{\infty}\}, \tag{5.4}$$

the expansion in series of $\widetilde{P}_{ij}(s)$ is

$$\widetilde{P}_{ij}(s) = P_j^{\infty} \frac{1}{(1-e^{-s})} + \sum_{n=0}^{\infty} (-1)^n R_{ij}^{(n)} \frac{s^n}{n!} \; . \tag{5.5}$$

Introducing this result into Eq. (5.2), the MFPT is obtained

$$\langle T_{ij} \rangle = \frac{1}{P_j^{\infty}} \left[R_{jj}^{(0)} - R_{ij}^{(0)} + \delta_{ij} \right]. \tag{5.6}$$

In Eq. (5.6), there are three different terms: the mean first return time $\langle T_{ii} \rangle = 1/P_i^{\infty}$, the quantity

$$\tau_j \equiv R_{jj}^{(0)}/P_j^{\infty}, \tag{5.7}$$

which is a time independent of the initial node and the time $R_{ij}^{(0)}/P_j^{\infty}$ that depends on i and j. Furthermore, from the detailed balance condition we obtained $\frac{R_{ij}^{(n)}}{P_j^{\infty}} = \frac{R_{ji}^{(n)}}{P_i^{\infty}}$, and thus

$$\langle T_{ij} \rangle - \langle T_{ji} \rangle = \tau_j - \tau_i, \tag{5.8}$$

which is a relation that describes the asymmetry of the dynamics [21]. The time τ_i is interpreted as the average time needed to reach the node i from a randomly chosen initial node of the network; on the other hand, the quantity $C_i \equiv \tau_i^{-1}$ is the random walk centrality introduced for the analysis of random walks with local information [21]. The centrality C_i combines information of the network and the random walk dynamics implemented to visit nodes and gives a high value to nodes that are easy to reach and a small values to nodes for which the random walker takes, in average, many steps to hit the node for the first time, starting from any node of the network [21, 30].

Additional to the times $\langle T_{ij}\rangle$ and τ_i, from Eq. (5.6), we have

$$\sum_{j=1}^{N}\langle T_{ij}\rangle P_j^{\infty} = \sum_{j=1}^{N} R_{jj}^{(0)} - \sum_{j=1}^{N} R_{ij}^{(0)} + 1 = \sum_{j=1}^{N} R_{jj}^{(0)} + 1. \tag{5.9}$$

The quantity $K \equiv \sum_{m=1}^{N} R_{mm}^{(0)}$ in the context of stochastic processes is called Kemeny's constant [132, 133]. As a consequence of Eq. (5.9), we have

$$K = \sum_{m=1}^{N} R_{mm}^{(0)} = \sum_{j\neq i}\langle T_{ij}\rangle P_j^{\infty}. \tag{5.10}$$

This result establishes a relation between the Kemeny's constant of Markovian processes and the global time obtained by averaging the mean first passage times $\langle T_{ij}\rangle$ weighted with the stationary distribution P_j^{∞}.

5.2 *Linear algebra approach*

In this section, we explore a general approach that allows us to study random walk models by using the information in the transition probability matrix Π in Eq. (2.2). We deduce expressions for the MFPT $\langle T_{ij}\rangle$, the time τ_i and the Kemeny's constant K in terms of the eigenvalues and eigenvectors of the transition matrix Π.

In order to calculate τ_i and $\langle T_{ij}\rangle$, it is necessary to find $P_{ij}(t)$. We start with the matrix form of Eq. (2.1)

$$\vec{P}(t) = \vec{P}(0)\Pi^t. \tag{5.11}$$

Here, $\vec{P}(t)$ is the probability vector at time t. Using Dirac's notation

$$P_{ij}(t) = \langle i|\,\Pi^t\,|j\rangle\,, \tag{5.12}$$

where $\{|m\rangle\}_{m=1}^{N}$ represents the canonical base of $\mathbb{R}^N$.

Due to the existence of a detailed balance condition, the matrix Π can be diagonalized and its spectrum has real values [5]. For right eigenvectors of Π we have $\Pi\,|\phi_i\rangle = \lambda_i\,|\phi_i\rangle$ for $i = 1, .., N$, where the set of eigenvalues is ordered in the form $\lambda_1 = 1$ and $1 > \lambda_2 \geq ... \geq \lambda_N \geq -1$. On the other hand, from right eigenvectors we define a matrix $\mathbf{Z}$ with elements $Z_{ij} = \langle i|\phi_j\rangle$. The matrix $\mathbf{Z}$ is invertible, and a new set of vectors $\langle\bar{\phi}_i|$ is obtained by means of $(\mathbf{Z}^{-1})_{ij} = \langle\bar{\phi}_i|j\rangle$, then

$$\delta_{ij} = (\mathbf{Z}^{-1}\mathbf{Z})_{ij} = \sum_{l=1}^{N}\langle\bar{\phi}_i|l\rangle\langle l|\phi_j\rangle = \langle\bar{\phi}_i|\phi_j\rangle \tag{5.13}$$

and

$$\mathbb{I} = \mathbf{Z}\mathbf{Z}^{-1} = \sum_{l=1}^{N} |\phi_l\rangle \left\langle \bar{\phi}_l \right|, \tag{5.14}$$

where $\mathbb{I}$ is the $N \times N$ identity matrix.

In different cases, especially when it is necessary to calculate numerically the eigenvalues and eigenvectors of the transition matrix, it is convenient to use the symmetry of the matrix of weights Ω. In this way, the eigenvectors $|\phi_l\rangle$ and $\left\langle \bar{\phi}_l \right|$ can alternatively be deduced from the analysis of the symmetric matrix $\mathbf{M}$ with elements

$$M_{ij} = \Omega_{ij}/\sqrt{S_i S_j}. \tag{5.15}$$

From an orthonormal set of eigenvectors $|\varphi_l\rangle$ that satisfy $\mathbf{M}\,|\varphi_l\rangle = \lambda_l\,|\varphi_l\rangle$ for $l = 1, \ldots, N$, it is obtained $|\phi_l\rangle = \mathbf{S}^{-1/2}\,|\varphi_l\rangle$ and $\left\langle \bar{\phi}_l \right| = \langle \varphi_l|\,\mathbf{S}^{1/2}$ where $\mathbf{S}$ is the $N \times N$ diagonal matrix $\mathbf{S} = \mathrm{diag}(S_1, \ldots, S_N)$.

Once the spectrum and the left and right eigenvectors of the transition matrix are obtained, we can deduce different analytical expressions for quantities that characterize the random walker. By using the diagonal matrix $\Delta \equiv \mathrm{diag}(\lambda_1, \ldots, \lambda_N)$, we obtained $\Pi = \mathbf{Z}\Delta\mathbf{Z}^{-1}$, therefore Eq. (5.12) takes the form

$$P_{ij}(t) = \langle i|\,\mathbf{Z}\Delta^t\mathbf{Z}^{-1}\,|j\rangle = \sum_{l=1}^{N} \lambda_l^t\,\langle i|\phi_l\rangle \left\langle \bar{\phi}_l|j \right\rangle. \tag{5.16}$$

From Eq. (5.16), the stationary probability distribution is $P_j^{\infty} = \langle i|\phi_1\rangle \left\langle \bar{\phi}_1|j \right\rangle$, where the result $\langle i|\phi_1\rangle =$ constant makes P_j^{∞} independent of the initial condition. Now, by means of the definition of $R_{ij}^{(0)}$, we have

$$R_{ij}^{(0)} = \sum_{l=2}^{N} \frac{1}{1-\lambda_l}\,\langle i|\phi_l\rangle \left\langle \bar{\phi}_l|j \right\rangle. \tag{5.17}$$

Therefore, the time τ_i is given by

$$\tau_i = \sum_{l=2}^{N} \frac{1}{1-\lambda_l} \frac{\langle i|\phi_l\rangle \left\langle \bar{\phi}_l|i \right\rangle}{\langle i|\phi_1\rangle \left\langle \bar{\phi}_1|i \right\rangle}, \tag{5.18}$$

and, for $i \neq j$ in Eq. (5.6), the MFPT $\left\langle T_{ij} \right\rangle$ is

$$\left\langle T_{ij} \right\rangle = \sum_{l=2}^{N} \frac{1}{1-\lambda_l} \frac{\langle j|\phi_l\rangle \left\langle \bar{\phi}_l|j \right\rangle - \langle i|\phi_l\rangle \left\langle \bar{\phi}_l|j \right\rangle}{\langle j|\phi_1\rangle \left\langle \bar{\phi}_1|j \right\rangle}, \tag{5.19}$$

whereas $\langle T_{ii}\rangle = (\langle i|\phi_1\rangle \left\langle \bar{\phi}_1|i \right\rangle)^{-1}$. Finally, from Eqs. (5.10) and (5.17), we obtained the Kemeny's constant

$$K = \sum_{m=1}^{N}\sum_{l=2}^{N} \frac{1}{1-\lambda_l} \left\langle \bar{\phi}_l|m \right\rangle \langle m|\phi_l\rangle = \sum_{l=2}^{N} \frac{1}{1-\lambda_l} \tag{5.20}$$

a result that only depends on the eigenvalues of the transition matrix Π.

5.3 *Global characterization*

In this section, we define global times that quantify the capacity of a random walk to reach any site of the network. By using these global times it is possible to compare different dynamics defined through Eq. (2.2). Global quantities like entropy rates [72, 134], the global mean first passage time [22] and the cover time [14, 16] have been used to study random walks on networks. We use the global quantity [30]

$$\tau \equiv \frac{1}{N}\sum_{i=1}^{N}\tau_i\,, \tag{5.21}$$

that gives an estimate of the average time to reach any site of the network. The values τ_i can present a huge dispersion due to the fact that in some irregular networks there are nodes easily accessible to the random walker and other sites that are hardly reached; despite this fact, the mean value of the times τ_i is an important quantity that characterize the capacity of a random walker to visit the nodes of a network. In the following section we explore the time τ for different random walk strategies.

In the particular case of random walks on weighted networks for which the value $S_i = \sum_{l=1}^{N}\Omega_{il}$ is constant, the stationary distribution given by Eq. (2.6) is $P_i^{\infty} = 1/N$. In this type of regular cases, using Eqs. (5.18) and (5.21) we have for the global time τ

$$\tau_{\text{reg}} = \frac{1}{N}\sum_{i=1}^{N}\frac{R_{ii}^{(0)}}{P_i^{\infty}} = \sum_{i=1}^{N}R_{ii}^{(0)} = \sum_{l=2}^{N}\frac{1}{1-\lambda_l}. \tag{5.22}$$

Then, in regular cases τ_{reg} is equal to the Kemeny's constant. Examples of this simplification are the normal random walks on a complete graph. This case illustrates the best scenario for the exploration of a network by means of normal random walks since all the nodes are connected. For a complete graph $A_{ij} = 1 - \delta_{ij}$ and $\pi_{i\to j} = \frac{1-\delta_{ij}}{N-1}$ [15]. The eigenvalues of the matrix Π are $\lambda_1 = 1$ and $\lambda_2 = \ldots = \lambda_N = -(N-1)^{-1}$, then the Kemeny's constant given by Eq. (5.22) for unbiased random walks on a complete network is

$$\tau_0 = \frac{(N-1)^2}{N}, \tag{5.23}$$

and this τ_0 is the lowest value that the time τ can take.

6. MFPTs and global times for particular dynamics

In this section, we apply the results in Eqs. (5.18)–(5.20) that allow to calculate exact values of $\langle T_{ij}\rangle$, τ_j and K for random walks on weighted networks. In particular, we analyse the global time τ and the Kemeny's constant for the preferential navigation, the Lévy flights on networks, the fractional transport and the model in Eq. (4.5). All these are defined in terms of a matrix of weights through the approach presented in Sections 3 and 4. Similar methods can be implemented to study different types of random walks described in Table 1.

6.1 *Preferential navigation*

The preferential navigation defined in Eq. (3.2) can represent different types of local random walkers; in particular, degree biased random walkers with transitions described in Section 3.3. In order to characterize

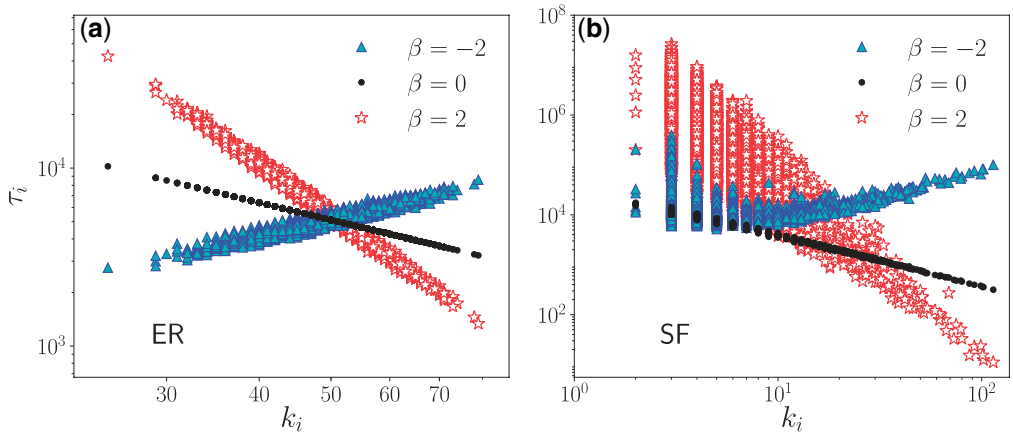

FIG. 9. Time τ_i vs. k_i for degree biased random walks on networks obtained using Eq. (5.18). (a) ER network with $N = 5000$ and $\langle k \rangle = 50$. (b) SF network with $N = 5000$, $\langle k \rangle = 6$. We use three values of the parameter β.

this process, in Fig. 9, we depict the values of the time τ_i for two different networks; the respective stationary distribution was presented in Fig. 2. The values that we obtained for τ_i give the average number of steps needed by a degree biased random walker to reach the node i from a random site in the network for different values of the parameter β. In the ER network, we observed the validity of the result $\tau_i \approx 1/P_i^{\infty}$ obtained by a mean field approximation [20]. On the other hand, in the SF network this approximation is not valid and it is observed that, compared with the case $\beta = 0$ that recovers the normal random walk, any degree biased random walk is a bad choice to reach efficiently nodes with a lower degree in the SF network. Our findings also reveal that, in comparison with the result for $\beta = 0$, in the ER network the value $\beta = -2$ reduces the number of steps needed to reach nodes with few connections, whereas the parameter $\beta = 2$ reduces the value of τ_i in nodes with large degree k_i.

Now, we calculate the global time τ for different cases of the preferential navigation defined by Eq. (3.2). We start generating the network and obtaining the transition matrix Π for specific values of the parameter β using the definition in Eq. (3.2). Once we obtained Π, we calculate the respective left and right eigenvectors $\langle \bar{\phi}_l |$ and $|\phi_l\rangle$ by the method described in Section 5.2. Then, we use the Eq. (5.18) to calculate the values of τ_i and finally, the mean value of the times τ_i gives τ. In a similar way, the Kemeny's constant is obtained from the spectrum of Π by means of Eq. (5.20). This process is repeated for different types of local models. We study cases for which the value q_i in Eq. (3.2) is determined by common quantities used to describe the role of the node i in each network; we explore the effect of the following q_i choices given by:

- The node degree k_i, therefore, the dynamics is the degree biased random walk explored in Figs. 2 and 9.
- The average degree of the neighbours of i given by $k_i^{(nn)} = (\sum_{l=1}^{N} A_{il} k_l)/k_i$. In this case, the transition probabilities $\pi_{i \to j}$ depend on the average degree of the first neighbours of the node j.
- The closeness centrality g_i of the node i given by $g_i = (\sum_{j \neq i} d_{ij})^{-1}$ where d_{ij} is the distance between i and j [13].

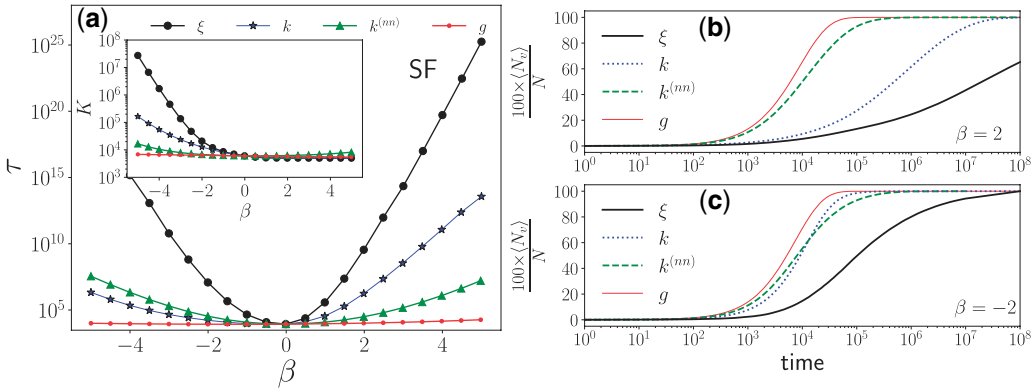

FIG. 10. Preferential random walks on a scale-free network (SF) of the Barabási–Albert type with $N = 5000$ nodes. (a) Global time τ vs. β for different types of random walks defined by Eq. (3.2) with q_i given by the node degree k_i, the average degree of neighbours $k_i^{(nn)}$, the closeness centrality g_i and the eigenvector centrality ξ_i; in the inset we plot the values of the Kemeny's constant K vs. β. The continuous lines are used as a guide. In (b) and (c), we present Monte Carlo simulations of the number of visited sites N_v as a function of time for node biased random walks with $\beta = -2$ and $\beta = 2$. The average of the number of visited nodes $\langle N_v\rangle$ is obtained from 1000 different realizations of the random walker. The results are expressed as a fraction of the total number of nodes multiplied by 100.

- The eigenvector centrality ξ_i of the node i. For the particular case $\beta = 1$, the probabilities $\pi_{i\to j}$ are determined by Eq. (3.6) that defines a maximal entropy random walk.

From the quantities k_i, $k_i^{(nn)}$, g_i and ξ_i, we analyse the global time τ for the preferential random walk with different values of the parameter β that modulates the biased random walk. From the numerical value of τ, we can compare the capacity of the dynamics to visit the nodes on the network. In Fig. 10, we analyse each of these models in a scale-free network. In Fig. 10(a), we depict the time τ as a function of β. In this case, we observe that unbiased random walks ($\beta = 0$) have the lowest values of τ. In addition, for the random walk with $q_i = g_i$ the values of τ do not change significantly with variations of the parameter β. It is observed that, for a given value of β, the random walk defined by $q_i = \xi_i$ has the largest values of τ, making this method to visit the nodes of the network inefficient to reach easily any node of the structure. The results reveal that, in comparison to the unbiased case, some node biased random walks need much more time to explore the network.

Furthermore, we are interested in the values of K and τ as a measure of the capacity of the random walker to explore sites on the network. In this way, we use Monte Carlo simulations of each preferential random walk with the values $\beta = -2$ and $\beta = 2$. We depict the results in Fig. 10(b, c) for the average number of visited nodes $\langle N_v\rangle$ as a function of time. Based on our findings for τ, we know that in some cases, for example when $q_i = k_i$ or $q_i = \xi_i$, the average time τ is much bigger for $\beta = 2$ than the result obtained for $\beta = -2$. These findings, and the behaviour observed in the Monte Carlo simulations, are in agreement with the predictions that τ gives for the different orders of magnitude of the time needed to visit any node on the network. In contrast, the Kemeny's constant (presented in the inset in Fig. 10(a)) does not describe the results obtained with Monte Carlo simulations. In this way, we can infer that, for the preferential navigation, the eigenvectors of the transition matrix Π contain relevant information about the efficiency of the processes; by considering only the spectrum of Π this information is lost. This does

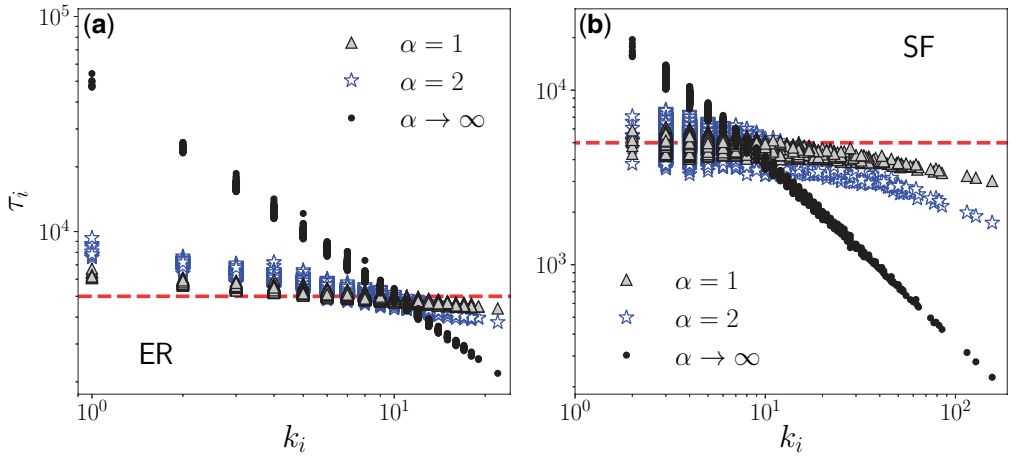

FIG. 11. Time τ_i vs. k_i for Lévy flights on networks; the quantities are obtained evaluating numerically Eq. (5.18). We use three values of the parameter α and we study two types of networks with $N = 5000$. (a) ER network at the connectivity threshold $p = (\log N)/N$. (b) SF network with $\langle k \rangle = 6$. Dashed lines denote the value τ_0 obtained for $\alpha = 0$.

not apply in the regular cases for which $P_i^{\infty} = 1/N$, where $\tau_{\text{reg}} = K$, and as a consequence important information to describe the efficiency of the process is contained in the spectrum of Π.

All the analysis discussed for the preferential random walk in Fig. 10 reveals that the time τ is a measure that describes globally the activity of random walks. On the other hand, the Kemeny's constant is a useful simplification to analyse only regular cases when the strength $S_i = \sum_{l=1}^{N} \Omega_{il}$ is constant.

6.2 *Lévy flights*

In this section, we analyse the efficiency of Lévy flights to explore a network. We use the formalism introduced in Section 5.2, which is valid for all the dynamics represented in terms of the matrix of weights Ω. In this way, we have exact analytical values that allow us to evaluate the mean first passage time $\langle T_{ij} \rangle$, the time τ_i and the global quantity τ by using Eqs. (5.18)–(5.21). In Fig. 11, we present the results for τ_i, as a function of k_i, for an ER network and a SF network. In a similar way to the results observed for the preferential random walk in Fig. 9, we obtained that for Lévy flights on these small-world networks $R_{ii}^{(0)} \approx 1$ and, as a consequence, $\tau_i \approx 1/P_i^{\infty}$.

On the other hand, the efficiency of Lévy flights can be explored with the quantity τ. In networks for which the long-range degree $D_i^{(\alpha)}$ is a constant for all the nodes on the network. The stationary distribution is $P_i^{\infty} = \frac{1}{N}$, that is, each node has the same probability to be visited in the limit $t \to \infty$. This is the case of some regular networks like rings, square lattices with periodic boundary conditions, complete graphs, among others. For this type of networks, τ is the Kemeny's constant given by Eq. (5.20), a result that only depends on the spectrum of the transition matrix Π, with elements given by Eq. (2.2). In the following part, we calculate analytically the value of τ for Lévy flights on rings, and we explore numerically other structures.

First, we study Lévy flights on a ring. In this particular case, the matrix of weights Ω and the transition matrix Π are circulant matrices [15]. The eigenvalues and eigenvectors of circulant matrices are well known [15, 135] and, in this way, we can obtain exact analytical expressions for the different quantities

presented in Section 5. For example, for a ring with an even number of nodes N, the spectrum of the transition matrix Π is

$$\lambda_l = \frac{2\sum_{n=1}^{N/2-1} n^{-\alpha}\cos\left[n\theta_l\right] + \left(\frac{N}{2}\right)^{-\alpha}\cos\left[\frac{N}{2}\theta_l\right]}{2\sum_{n=1}^{N/2-1} n^{-\alpha} + \left(\frac{N}{2}\right)^{-\alpha}}, \tag{6.1}$$

with $\theta_l = 2\pi(l-1)/N$. In a similar way, for an odd value of N, we have

$$\lambda_l = \frac{\sum_{n=1}^{(N-1)/2} n^{-\alpha}\cos\left[n\theta_l\right]}{\sum_{n=1}^{(N-1)/2} n^{-\alpha}}. \tag{6.2}$$

Introducing the eigenvalues in Eqs. (6.1) and (6.2) into the relation in Eq. (5.22), we obtain analytically the value of τ for Lévy flights on a ring. In particular, when $\alpha \to \infty$ we deduce τ for normal random walks on a ring

$$\tau = \sum_{l=2}^{N} \frac{1}{1-\cos\left[\frac{2\pi}{N}(l-1)\right]}. \tag{6.3}$$

In Fig. 12, we analyse the values of τ for Lévy flights on finite rings. In Fig. 12(a), we present the result for τ/τ_0 as a function of the ring size N for different values of α. We observe that, in the limit $\alpha \to \infty$, the time τ behaves as $\tau/\tau_0 \sim N$, therefore $\tau \sim N^2$. In a similar way, the reduction of the parameter α gradually changes τ to $\tau \sim N^{1+\delta}$, where δ takes values in the interval $0 < \delta < 1$ for $0 < \alpha < \infty$. Finally, in the limit $\alpha \to 0$, we have $\tau \sim N$. In addition, in Fig. 12(b), we depict the results for τ/τ_0 as a function of α for different values of the ring size N. In this case, it is observed how the relation τ/τ_0 maintains a similar behaviour for different values of the number of nodes N. In the interval $0 < \alpha < 2$, we observed that τ/τ_0 are close to the value τ_0 obtained in the limit $\alpha \to 0$ or in a complete graph. Moreover, in the range $2 < \alpha \leq 5$, τ/τ_0 shows an increase that can be of several orders of magnitude. For $\alpha > 6$, the results are again constant and close to the limit $\alpha \to \infty$ given by Eq. (6.3).

Once we analysed the Lévy flights on rings, for which the eigenvalues of the transition have the analytic form presented in Eqs. (6.1) and (6.2), it is important to explore the value of τ for other structures. In Fig. 13, we present the results obtained for the average number of steps τ as a function of the parameter α for Lévy flights on different types of networks. In regular networks (ring and square lattice), the value of τ is obtained from Eq. (5.22). For the tree, the ER and the SF networks, the results are calculated using Eqs. (5.18) and (5.21). The values obtained for τ suggest that, compared with the normal random walker, in large-world networks the average number of steps required to reach any node in the network is lower for the Lévy flight. In small-world networks, the differences are smaller, but even in this case, the Lévy dynamics improve the results obtained for the normal random walker. This result is reasonable due to the fact that in large-world networks, Lévy flights define a model that induces the small-world property. In the case of small-world networks, the nodes in the network are separated by short distances and, in this way, Lévy flights and the normal random walk explore the network with times τ of the same order of magnitude [30].

6.3 *Fractional transport*

In this section, we apply the approach described before for preferential random walks and Lévy flights to the case of the fractional transport on networks with transition probabilities between nodes given by the

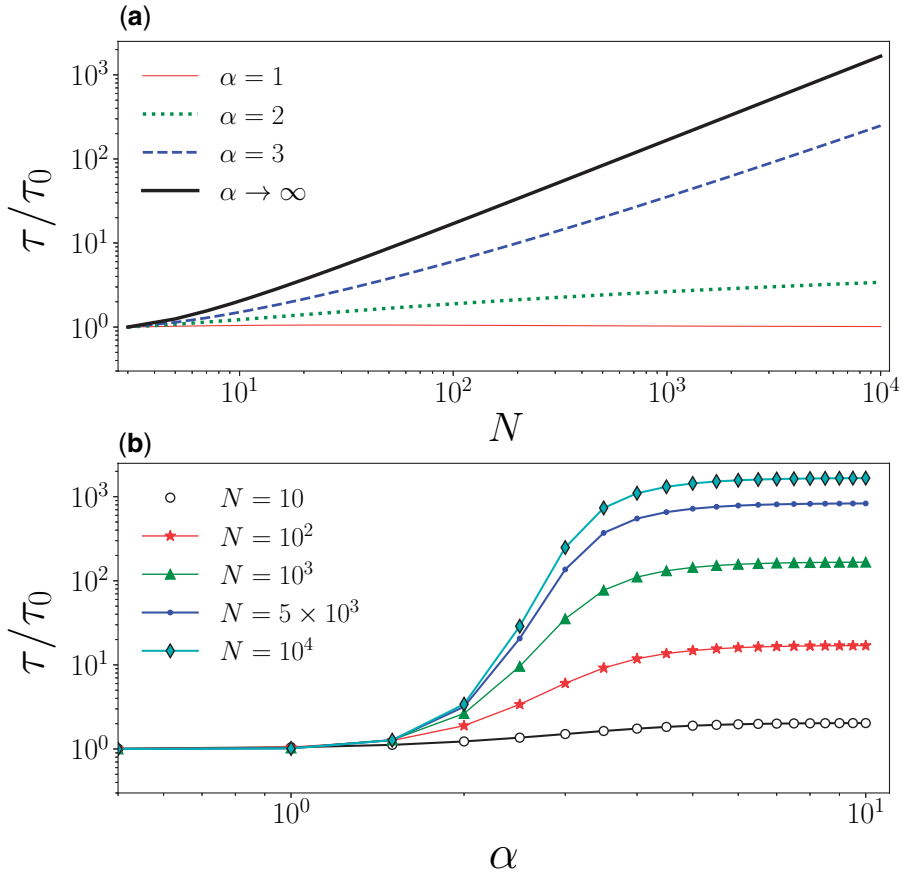

FIG. 12. Global time τ for Lévy flights to reach any site of a finite ring. The results are expressed in terms of the value $\tau_0 = (N-1)^2/N$ obtained for a complete graph. The values are calculated using the analytical expressions for the spectra in Eqs. (6.1)-(6.2) and the Eq. (5.22). In (a) the time τ is presented as a function of N for $\alpha = 1, 2, 3$ and the limit case $\alpha \to \infty$; these results are complemented in (b) where the time τ is plotted as a function of α for Lévy flights with different values of N.

Eq. (4.11). In the case of rings with N nodes, the eigenvalues of the transition matrices can be obtained analytically [40, 56]. For this regular structure, the fractional degree in Eq. (4.10) is a constant $k^{(\gamma)}$ given by [56]

$$k^{(\gamma)} = (\mathbf{L}^{\gamma})_{ii} = \frac{1}{N}\sum_{l=1}^{N}\left(2 - 2\cos\left[\frac{2\pi}{N}(l-1)\right]\right)^{\gamma} \tag{6.4}$$

and the eigenvalues $\{\lambda_i\}_{i=1}^{N}$ for the transition matrix Π, with elements in Eq. (4.11), are

$$\lambda_i = 1 - \frac{1}{k^{(\gamma)}}\left(2 - 2\cos\left[\frac{2\pi}{N}(i-1)\right]\right)^{\gamma}. \tag{6.5}$$

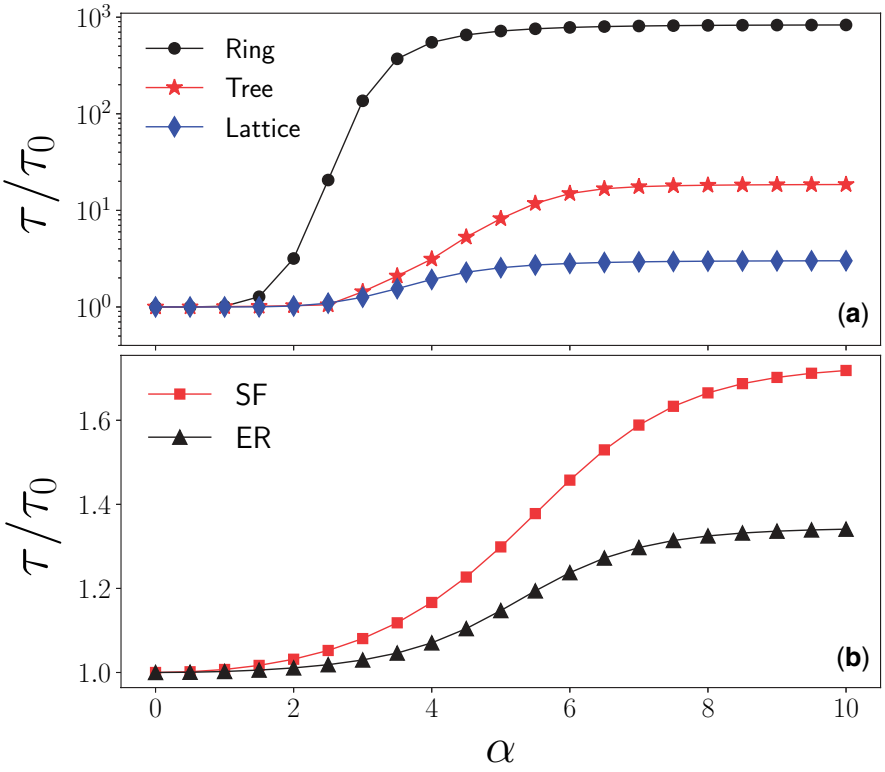

FIG. 13. Global time τ that gives the average number of steps needed for Lévy flights to reach any site of the network in different structures; the results are expressed in terms of the value $\tau_0 = (N-1)^2/N$. In (a) and (b), we depict the time τ for different values of α in networks with $N = 5000$. We calculated the values numerically using the Eqs. (5.18) and (5.21) for large-world networks (ring, tree and a square lattice of size 50×100 and periodic boundary conditions) and small-world networks (ER network in the connectivity threshold and a SF network of the Barabási–Albert type).

Now, as a consequence of the results in Eqs. (6.4) and (6.5), the time τ that characterizes the random walk in Eq. (4.11) to explore a ring coincides with the Kemeny's constant and is given by [56]

$$\tau = k^{(\gamma)} \sum_{m=2}^{N} \frac{1}{(2-2\cos\phi_m)^{\gamma}}, \tag{6.6}$$

where $\phi_i \equiv \frac{2\pi}{N}(i-1)$.

In Fig. 14, we represent the numerical values of the global time τ/τ_0 obtained for the fractional transport on rings. The results are calculated by direct evaluation of the result in Eq. (6.6). We explore the parameter γ that defines the fractional transport for different values of the size of the ring N. In Fig. 14, we observe that the dynamics with $0 < \gamma < 1$ always improves the capacity to explore the ring in comparison with a normal random walk recovered in the case $\gamma = 1$. This effect is observed in the reduction of the quantity τ/τ_0 for $\gamma = 0.25$, 0.5 and $\gamma = 0.75$. On the other hand, in the limit $\gamma \to 0$ the movement is equivalent to a normal random walker on a fully connected network allowing, with the

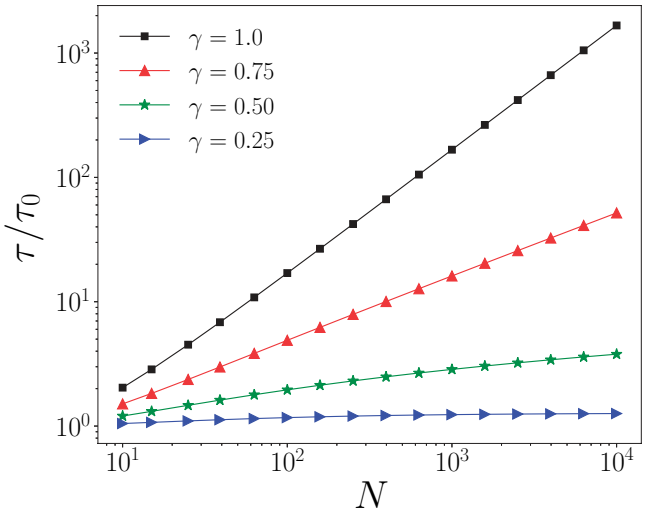

FIG. 14. Global time τ as a function of the number of nodes N for the fractional transport on rings. We obtain the results for the time τ by direct evaluation of the Eq. (6.6). We express the time τ in relation to $\tau_0 = (N-1)^2/N$ for different values of the parameter γ that defines each random walk. Solid lines are used as a guide.

same probability, transitions from one node to any site of the ring [40]. A similar behaviour to this limit is also observed for the case $\gamma = 0.25$ for all the values of N analysed.

Through the evaluation of the global time τ, we can analyse the fractional dynamics in different types of large-world and small-world networks. Unlike the previous cases explored for rings, other types of networks have not the same fractional degree $k_i^{(\gamma)}$ for all the nodes $i = 1, 2, \ldots, N$. In this way, the capacity of the random walker to visit all the nodes of the network is quantified by the time τ given by the average of the times Eq. (5.18) that depends on the eigenvectors and eigenvalues of the transition matrix Π with elements given by Eq. (4.11).

In Fig. 15, we show the global time τ for networks with $N = 5000$ nodes. We analyse a deterministic tree created by an iterative method for which an initial node ramifies with two leaves that also repeat this process until the size N. The final structure is a large-world network with average distances $\langle d \rangle$ between nodes that scale as the size of the network. On the other hand, we analyse random networks generated with the Watts–Strogatz model for which an initially regular network is generated and then rewired with probability p taken from a uniform distribution; for values of $p \to 0$ this random network has the large world property of the original lattice; however, the rewiring introduces shortcuts that reduce the average path lengths with the increasing of p [136]. In addition, small-world networks generated with the ER model and a SF network of the Barabási–Albert type are explored [137, 138]. We observe that the generalized transport defined in terms of the fractional graph Laplacian $\mathbf{L}^\gamma$ with $0 < \gamma < 1$ always improves the efficiency to explore the networks, the effects are marked in large-world networks with a significant change in the value τ/τ_0, but the dynamics also improves the results for small-world networks.

As we discussed in Section 4.3, the random walk defined in terms of the fractional graph Laplacian $\mathbf{L}^\gamma$ is a particular case of non-local strategies expressed using functions of the Laplacian $g(\mathbf{L})$. The same approach presented here applies to other types of dynamics [56]; for example, when we use weights defined in terms of the logarithmic function $\log(\mathbb{I} + \alpha\mathbf{L})$ for $\alpha > 0$ and the function $\mathbb{I} - e^{-a\mathbf{L}}$ with $a > 0$.

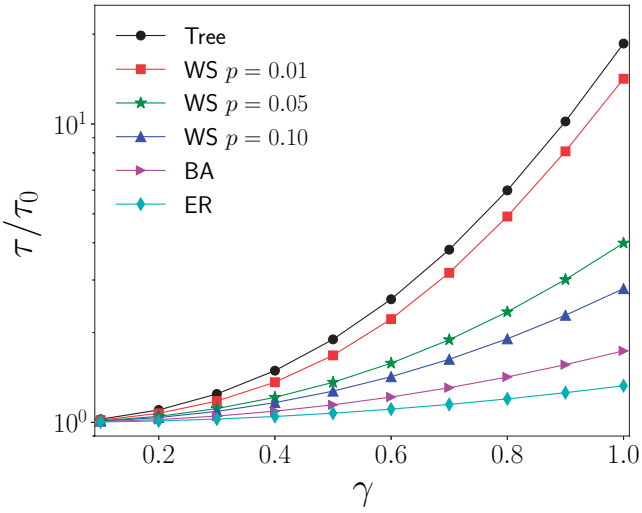

FIG. 15. Global time τ for the fractional transport on connected networks with $N = 5000$ nodes: a tree, random networks generated from the Watts–Strogatz (WS) model with rewiring probabilities $p = 0.01, p = 0.05, p = 0.1$, a SF network of the Barabási–Albert type and a random network of the ER type with $p = \log N/N$. We obtain the results for the time τ by numerical evaluation of the Eqs. (5.18) and (5.21). We express τ in relation to the value $\tau_0 = (N-1)^2/N$. Solid lines are used as a guide.

6.4 *Random walks to visit specific locations*

We end this section with an application of the formalism developed in terms of a matrix of weights but now for a model in the context of human mobility that does not necessarily require the definition of a network. We analyse the random walk model with transition probabilities defined by Eqs. (4.5)–(4.6) to visit specific locations in a region. In this case, the matrix of weights with elements $\Omega_{ij}^{(\alpha)}(R)$ depends on the characteristic length R, that defines a local neighbourhood, and the parameter α that controls a dynamics with similar characteristics to the Lévy flights on networks but now to visit the locations. In order to quantify the capacity of the random walker to visit the N locations in space, we use the time $\tau^{(\alpha)}(R)$, that gives the average number of steps needed to reach any of the N sites independently of the initial condition by numerical evaluation of the Eqs. (5.18) and (5.21). In Fig. 16, we present the time $\tau^{(\alpha)}(R)$ for different values of the parameters α and R to visit $N = 100$ random locations on the continuous two-dimensional plane. The values are obtained using the exact analytical results in terms of the eigenvectors and eigenvalues of the transition matrix defined by Eq (4.5). It is observed how, for $\alpha \gg 1$, different values of R define diverse ways to visit the N sites in the plane; in particular, $R \ll 1$ characterizes a local movement that requires many steps to reach the locations. Models with $\alpha \leq 1$ are optimal and in this interval the results are independent of the parameter R. The results observed with the help of the global time $\tau^{\alpha}(R)$ suggest that long-range dynamics always improve the capacity of the random walker to reach any of the N locations [28].

7. Conclusions

In this work, we presented a survey of a general approach to analyse random walks on undirected weighted networks. These random walks are described as a discrete-time Markovian process with transition probabilities defined in terms of a symmetric matrix of weights. We consider in this survey both local and

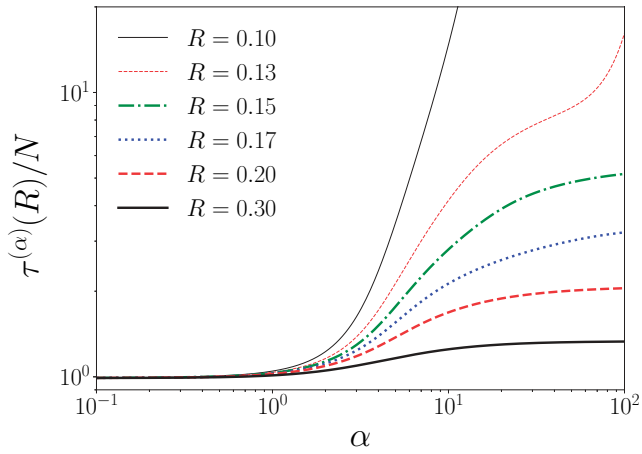

FIG. 16. Global time to visit N locations. The value $\tau^{(\alpha)}(R)$ gives the average number of steps needed to reach any of the N sites, independently of the initial condition; we use $N = 100$ random sites in the region $[0, 1] \times [0, 1]$ in $\mathbb{R}^2$. The results are obtained from the analytical expressions in Eqs. (5.18)–(5.21) and the numerical evaluation of the eigenvectors and eigenvalues of the transition matrix with elements $w_{i\to j}^{(\alpha)}(R)$.

non-local dynamics: however, the emphasis is on non-local random walks on networks, since this long-range dynamics is more general and includes the local random walks as a particular case. Besides this, it is only recently that these non-local stochastic processes on networks have started to being explored in detail.

We start with an introduction to random walks on weighted networks and briefly point out its relevance in many fields: mathematics, physics, biology, economics, finance, computer science, among others. Then, we present a general formalism of random walks on networks based on discrete-time master equations and transition probabilities. Firstly, we study local random walk models, including the normal random walk, biased random walks with preferential navigation, random walks for image segmentation, and maximal entropy random walks. Secondly, we analyse non-local random walk models, starting with a discussion of Lévy-like dynamics on networks. Then, we discuss an application of the non-local formalism to the case of spatial networks and human mobility; in particular the gravity law model of mobility and migration.

Finally, we study in detail the important formalism of the fractional graph Laplacian, introduced by the authors some years ago, that incorporates, for the first time, the ideas of fractional dynamics and fractional calculus to network science. This formalism is based on the spectral properties of the Laplacian matrix and is very general and easy to implement. In the last two sections of this survey, we address the problem of the mean first passage time in networks and the global characterization of the dynamics to explore the whole network. We summarize in a table the local and non-local dynamics with the different weighted matrices for each model, including the corresponding references studying each strategy.

We hope that this survey, which does not pretend to encompass the vast literature of random walks and network science and focuses on the interplay between local and non-local random walks on networks, can be useful and stimulate further study in this important area of research.

Funding

This work was supported by Universidad Nacional Autónoma de México - Programa de Apoyo a Proyectos de Investigación e Innovación Tecnológica - IN116220.

References

1. Klafter, J. & Sokolov, I. (2011) *First Steps in Random Walks: From Tools to Applications*. Oxford: Oxford University Press.
2. Masuda, N., Porter, M. A. & Lambiotte, R. (2017) Random walks and diffusion on networks. *Phys. Rep.*, **716–717**, 1–58.
3. Ibe, O. C. (2013) *Elements of Random Walk and Diffusion Processes*, 1st edn. New Jersy: Wiley Publishing.
4. Redner, S. (2001) *A Guide to First-Passage Processes*. New York: Cambridge University Press.
5. van Kampen, N. G. (1992) *Stochastic Processes in Physics and Chemistry*. The Netherlands: North Holland.
6. Viswanathan, G. M., da Luz, M. G. E., Raposo, E. P. & Stanley, H. E. (2011) *The Physics of Foraging*. New York: Cambridge University Press.
7. Weiss, G. H. (1994) *Aspects and Applications of the Random Walk*. Amsterdam: North-Holland.
8. Barabási, A.-L. & Pósfai, M. (2016) *Network Science*. Cambridge: Cambridge University Press.
9. Caldarelli, G. (2007) *Scale-Free Networks: Complex Webs in Nature and Technology*. Oxford, UK: Oxford University Press.
10. Dorogovtsev, S. & Mendes, J. (2003) *Evolution of Networks: From Biological Nets to the Internet and WWW*. Oxford, UK: Oxford University Press.
11. Estrada, E. (2011) *The Structure of Complex Networks: Theory and Applications*. Oxford, UK: Oxford University Press.
12. Latora, V., Nicosia, V. & Russo, G. (2017) *Complex Networks: Principles, Methods and Applications*. Cambridge: Cambridge University Press.
13. Newman, M. E. J. (2010) *Networks: An Introduction*. Oxford: Oxford University Press.
14. Barrat, A., Barthélemy, M. & Vespignani, A. (2008) *Dynamical Processes on Complex Networks*. Cambridge: Cambridge University Press.
15. Van Mieghem, P. (2011) *Graph Spectra for Complex Networks*. New York: Cambridge University Press.
16. Hughes, B. D. (1996) *Random Walks and Random Environments: Vol. 1: Random Walks*. New York: Oxford University Press.
17. Lovász, L. (1996) Random walks on graphs: a survey. *Combinatorics, Paul Erdős is Eighty* (D. Miklós, V. T. Sós & T. Szőnyi, eds), vol. 2, Budapest: János Bolyai Mathematical Society, pp. 353–398.
18. Mülken, O. & Blumen, A. (2011) Continuous-time quantum walks: models for coherent transport on complex networks. *Phys. Rep.*, **502**, 37–87.
19. Alessandretti, L., Sun, K., Baronchelli, A. & Perra, N. (2017) Random walks on activity-driven networks with attractiveness. *Phys. Rev. E*, **95**, 052318.
20. Fronczak, A. & Fronczak, P. (2009) Biased random walks in complex networks: the role of local navigation rules. *Phys. Rev. E*, **80**, 016107.
21. Noh, J. D. & Rieger, H. (2004) Random walks on complex networks. *Phys. Rev. Lett.*, **92**, 118701.
22. Tejedor, V., Bénichou, O. & Voituriez, R. (2009) Global mean first-passage times of random walks on complex networks. *Phys. Rev. E*, **80**, 065104.
23. De Domenico, M., Granell, C., Porter, M. A. & Arenas, A. (2016) The physics of spreading processes in multilayerÂ networks. *Nat. Phys.*, **12**, 901.
24. Durrett, R. (2010) Some features of the spread of epidemics and information on a random graph. *Proc. Natl. Acad. Sci. USA*, **107**, 4491–4498.
25. Pastor-Satorras, R., Castellano, C., Van Mieghem, P. & Vespignani, A. (2015) Epidemic processes in complex networks. *Rev. Mod. Phys.*, **87**, 925–979.
26. Sarkar, P. & Moore, A. W. (2011) *Random Walks in Social Networks and their Applications: A Survey*. Boston: Springer, pp. 43–77.
27. Blanchard, P. & Volchenkov, D. (2011) *Random Walks and Diffusions on Graphs and Databases. An Introduction*. Springer Series in Synergetics. Berlin: Springer.
28. Riascos, A. P. & Mateos, J. L. (2017) Emergence of encounter networks due to human mobility. *PLoS One*, **12**, e0184532.

29. Riascos, A. P. & Mateos, J. L. (2020) Networks and long-range mobility in cities: a study of more than one billion taxi trips in New York City. *Sci. Rep.*, **10**, 4022.

30. Riascos, A. P. & Mateos, J. L. (2012) Long-range navigation on complex networks using Lévy random walks. *Phys. Rev. E*, **86**, 056110.

31. Guo, Q., Cozzo, E., Zheng, Z. & Moreno, Y. (2016) Lévy random walks on multiplex networks. *Sci. Rep.*, **6**, 37641.

32. Huang, W., Chen, S. & Wang, W. (2014) Navigation in spatial networks: a survey. *Phys. A: Stat. Mech. Appl.*, **393**, 132–154.

33. Weng, T., Small, M., Zhang, J. & Hui, P. (2015) Lévy walk navigation in complex networks: a distinct relation between optimal transport exponent and network dimension. *Sci. Rep.*, **5**, 17309.

34. Weng, T., Zhang, J., Khajehnejad, M., Small, M., Zheng, R. & Hui, P. (2016) Navigation by anomalous random walks on complex networks. *Sci. Rep.*, **6**, 37547.

35. Zhao, Y., Weng, T. & Huang, D. (2014) Lévy walk in complex networks: an efficient way of mobility. *Phys. A: Stat. Mech. Appl.*, **396**, 212–223.

36. Zheng, Z., Xiao, G., Wang, G., Zhang, G. & Jiang, K. (2017) Mean first passage time of preferential random walks on complex networks with applications. *Math. Probl. Eng.*, **2017**, 8217361.

37. Estrada, E., Delvenne, J.-C., Hatano, N., Mateos, J. L., Metzler, R., Riascos, A. P. & Schaub, M. T. (2018) Random multi-hopper model: super-fast random walks on graphs. *J. Compl. Net.*, **6**, 382–403.

38. Estrada, E. (2021) Path Laplacians versus fractional Laplacians as nonlocal operators on networks. *New J. Phys.*, **23**, 073049.

39. Riascos, A. P. & Mateos, J. L. (2014) Fractional dynamics on networks: Emergence of anomalous diffusion and Lévy flights. *Phys. Rev. E*, **90**, 032809.

40. Riascos, A. P. & Mateos, J. L. (2015) Fractional diffusion on circulant networks: emergence of a dynamical small world. *J. Stat. Mech.*, **2015**, P07015.

41. Allen-Perkins, A. & Andrade, R. F. S. (2019) Fractional dynamics on circulant multiplex networks: optimal coupling and long-range navigation for continuous-time random walks. *J. Stat. Mech.*, **2019**, 123302.

42. Benzi, M., Bertaccini, D., Durastante, F. & Simunec, I. (2020) Non-local network dynamics via fractional graph Laplacians. *J. Compl. Net.*, **8**, cnaa017.

43. de Nigris, S., Carletti, T. & Lambiotte, R. (2017) Onset of anomalous diffusion from local motion rules. *Phys. Rev. E*, **95**, 022113.

44. de Nigris, S., Hastir, A. & Lambiotte, R. (2016) Burstiness and fractional diffusion on complex networks. *Eur. Phys. J. B*, **89**, 114.

45. Michelitsch, T. M., Collet, B. A., Riascos, A. P., Nowakowski, A. F. & Nicolleau, F. C. G. A. (2016b) A fractional generalization of the classical lattice dynamics approach. *Chaos Solitons Fractals*, **92**(Supplement C), 43 – 50.

46. Michelitsch, T. M., Collet, B. A., Riascos, A. P., Nowakowski, A. F. & Nicolleau, F. C. G. A. (2017) Fractional random walk lattice dynamics. *J. Phys. A: Math. Theor.*, **50**, 055003.

47. Michelitsch, T. M., Collet, B. A., Riascos, A. P., Nowakowski, A. F. & Nicolleau, F. C. G. A. (2017) Recurrence of random walks with long-range steps generated by fractional Laplacian matrices on regular networks and simple cubic lattices. *J. Phys. A: Math. Theor.*, **50**, 505004.

48. Michelitsch, T. M., Riascos, A. P., Collet, B. A., Nowakowski, A. F. & Nicolleau, F. C. G. A. (2019) *Fractional Dynamics on Networks and Lattices*. London: ISTE/Wiley.

49. Bautista, E., Abry, P. & Goncalves, P. (2019) Lγ-PageRank for semi-supervised learning. *Appl. Netw. Sci.*, **4**, 57.

50. Chen, Y., Gel, Y. R. & Avrachenkov, K. (2020) LFGCN: Levitating over Graphs with Levy Flights. *2020 IEEE International Conference on Data Mining (ICDM)*, 2020, pp. 960–965.

51. de Nigris, S., Bautista, E., Abry, P., Avrachenkov, K. & Goncalves, P. (2017) Fractional graph-based semi-supervised learning. *2017 25th European Signal Processing Conference (EUSIPCO)*. pp. 356–360.

52. Riascos, A. P. & Mateos, J. L. (2015) Fractional quantum mechanics on networks: long-range dynamics and quantum transport. *Phys. Rev. E*, **92**, 052814.

53. González, F. H., Riascos, A. P. & Boyer, D. (2021) Diffusive transport on networks with stochastic resetting to multiple nodes. *Phys. Rev. E*, **103**, 062126.
54. Riascos, A. P., Boyer, D., Herringer, P. & Mateos, J. L. (2020) Random walks on networks with stochastic resetting. *Phys. Rev. E*, **101**, 062147.
55. Estrada, E. (2020) Fractional diffusion on the human proteome as an alternative to the multi-organ damage of SARS-CoV-2. *Chaos*, **30**, 081104.
56. Riascos, A. P., Michelitsch, T. M., Collet, B. A., Nowakowski, A. F. & Nicolleau, F. C. G. A. (2018) Random walks with long-range steps generated by functions of Laplacian matrices. *J. Stat. Mech.*, **2018**, 043404.
57. Condamin, S., Bénichou, O. & Moreau, M. (2007) Random walks and Brownian motion: a method of computation for first-passage times and related quantities in confined geometries. *Phys. Rev. E*, **75**, 021111.
58. Zhang, Z., Shan, T. & Chen, G. (2013) Random walks on weighted networks. *Phys. Rev. E*, **87**, 012112.
59. Telcs, A. (1989) Random walks on graphs, electric networks and fractals. *Probab. Theory Relat. Fields*, **82**, 435–449.
60. Kishore, V., Santhanam, M. S. & Amritkar, R. E. (2011) Extreme events on complex networks. *Phys. Rev. Lett.*, **106**, 188701.
61. Sanders, D. P. (2009) Exact encounter times for many random walkers on regular and complex networks. *Phys. Rev. E*, **80**, 036119.
62. Yang, S.-J. (2005) Exploring complex networks by walking on them. *Phys. Rev. E*, **71**, 016107.
63. Gao, L., Peng, J., Tang, C. & Riascos, A. P. (2021) Trapping efficiency of random walks on weighted scale-free trees. *J. Stat. Mech*, **2021**, 063405.
64. Meyer, B., Agliari, E., Bénichou, O. & Voituriez, R. (2012) Exact calculations of first-passage quantities on recursive networks. *Phys. Rev. E*, **85**, 026113.
65. Wang, W.-X., Wang, B.-H., Yin, C.-Y., Xie, Y.-B. & Zhou, T. (2006) Traffic dynamics based on local routing protocol on a scale-free network. *Phys. Rev. E*, **73**, 026111.
66. Kwon, S., Choi, W. & Kim, Y. (2010) Bimolecular chemical reactions on weighted complex networks. *Phys. Rev. E*, **82**, 021108.
67. Kishore, V., Santhanam, M. S. & Amritkar, R. E. (2012) Extreme events and event size fluctuations in biased random walks on networks. *Phys. Rev. E*, **85**, 056120.
68. Ling, X., Hu, M.-B., Ding, J.-X., Shi, Q. & Jiang, R. (2013) Effects of target routing model on the occurrence of extreme events in complex networks. *Eur. Phys. J. B*, **86**.
69. Battiston, F., Nicosia, V. & Latora, V. (2016) Efficient exploration of multiplex networks. *New J. Phys.*, **18**, 043035.
70. Lambiotte, R., Sinatra, R., Delvenne, J.-C., Evans, T. S., Barahona, M. & Latora, V. (2011) Flow graphs: interweaving dynamics and structure. *Phys. Rev. E*, **84**, 017102.
71. Zhang, Y., Zhang, Z., Guan, J. & Zhou, S. (2011) Diffusional annihilation processes in weighted scale-free networks with an identical degree sequence. *J. Stat. Mech.*, **2011**, P10001.
72. Burda, Z., Duda, J., Luck, J. M. & Waclaw, B. (2009) Localization of the Maximal Entropy Random Walk. *Phys. Rev. Lett.*, **102**, 160602.
73. Sinatra, R., Gómez-Gardeñes, J., Lambiotte, R., Nicosia, V. & Latora, V. (2011) Maximal-entropy random walks in complex networks with limited information. *Phys. Rev. E*, **83**, 030103.
74. Frank, L. R. & Galinsky, V. L. (2014) Information pathways in a disordered lattice. *Phys. Rev. E*, **89**, 032142.
75. Lin, Y. & Zhang, Z. (2014) Mean first-passage time for maximal-entropy random walks in complex networks. *Sci. Rep.*, **4**.
76. Ochab, J. K. (2012) Maximal-entropy random walk unifies centrality measures. *Phys. Rev. E*, **86**, 066109.
77. Grady, L. (2006) Random walks for image segmentation. *IEEE Trans. Pattern Anal. Mach. Intell.*, **28**, 1768–1783.
78. Zlatić, V., Gabrielli, A. & Caldarelli, G. (2010) Topologically biased random walk and community finding in networks. *Phys. Rev. E*, **82**, 066109.

79. Sinop, A. & Grady, L. (2007) A seeded image segmentation framework unifying graph cuts and random walker which yields a new algorithm. *IEEE 11th International Conference on Computer Vision, 2007. ICCV 2007*. pp. 1–8.

80. Brin, S. & Page, L. (1998) The anatomy of a large-scale hypertextual Web search engine. *Comput. Netw. ISDN Syst.*, **30**, 107–117.

81. Arias, J. H., Gómez-Gardenes, J., Meloni, S. & Estrada, E. (2018) Epidemics on plants: modeling long-range dispersal on spatially embedded networks. *J. Theor. Biol.*, **453**, 1–13.

82. Estrada, E. (2012) Path Laplacian matrices: introduction and application to the analysis of consensus in networks. *Linear Algebra Appl.*, **436**, 3373–3391.

83. Estrada, E. (2020) d-path Laplacians and quantum transport on graphs. *Mathematics*, **8**, 527.

84. Estrada, E., Hameed, E., Hatano, N. & Langer, M. (2017) Path Laplacian operators and superdiffusive processes on graphs. I. One-dimensional case. *Linear Algebra Appl.*, **523**, 307–334.

85. Estrada, E., Hameed, E., Langer, M. & Puchalska, A. (2018b) Path Laplacian operators and superdiffusive processes on graphs. II. Two-dimensional lattice. *Linear Algebra Appl.*, **555**, 373–397.

86. Martin, D., Fowlkes, C., Tal, D. & Malik, J. (2001) A database of human segmented natural images and its application to evaluating segmentation algorithms and measuring ecological statistics. *Proceedings of the Eighth IEEE International Conference on Computer Vision, 2001. ICCV 2001*, vol. 2. pp. 416–423.

87. Metzler, R. & Klafter, J. (2004) The restaurant at the end of the random walk: recent developments in the description of anomalous transport by fractional dynamics. *J. Phys. A: Math. Gen.*, **37**, R161.

88. Zaburdaev, V., Denisov, S. & Klafter, J. (2015) Lévy walks. *Rev. Mod. Phys.*, **87**, 483–530.

89. Boyer, D., Crofoot, M. C. & Walsh, P. D. (2012) Non-random walks in monkeys and humans. *J. R. Soc. Interface*, **9**, 842–847.

90. Boyer, D., Ramos-Fernández, G., Miramontes, O., Mateos, J. L., Cocho, G., Larralde, H., Ramos, H. & Rojas, F. (2006) Scale-free foraging by primates emerges from their interaction with a complex environment. *Proc. R. Soc. B*, **273**, 1743–1750.

91. Ramos-Fernández, G., Mateos, J. L., Miramontes, O., Cocho, G., Larralde, H. & Ayala-Orozco, B. (2004) Lévy walk patterns in the foraging movements of spider monkeys (*Ateles geoffroyi*). *Behav. Ecol. Sociobiol.*, **55**, 223–230.

92. Wosniack, M. E., Santos, M. C., Raposo, E. P., Viswanathan, G. M. & da Luz, M. G. E. (2017) The evolutionary origins of Lévy walk foraging. *PLoS Comput. Biol.*, **13**, e1005774.

93. Brockmann, D., Hufnagel, L. & Geisel, T. (2006) The scaling laws of human travel. *Nature (London)*, **439**, 462–465.

94. Brown, C., Liebovitch, L. & Glendon, R. (2007) Lévy flights in Dobe Ju/'hoansi foraging patterns. *Hum. Ecol.*, **35**, 129–138.

95. Rhee, I., Shin, M., Hong, S., Lee, K., Kim, S. J. & Chong, S. (2011) On the Levy-Walk nature of human mobility. *IEEE/ACM Trans. Netw.*, **19**, 630–643.

96. Metzler, R. & Klafter, J. (2000) The random walk's guide to anomalous diffusion: a fractional dynamics approach. *Phys. Rep.*, **339**, 1–77.

97. Barthélemy, M. (2011) Spatial networks. *Phys. Rep.*, **499**, 1 – 101.

98. Barbosa, H., Barthelemy, M., Ghoshal, G., James, C. R., Lenormand, M., Louail, T., Menezes, R., Ramasco, J. J., Simini, F. & Tomasini, M. (2018) Human mobility: models and applications. *Phys. Rep.*, **734**, 1 – 74.

99. Barthélemy, M. (2016) *The Structure and Dynamics of Cities: Urban Data Analysis and Theoretical Modeling*. Cambridge: Cambridge University Press.

100. Batty, M. (2013) *The New Science of Cities*. Cambridge:Cambridge, MA: MIT Press.

101. Melikov, P., Kho, J. A., Fighiera, V., Alhasoun, F., Audiffred, J., Mateos, J. L. & González, M. C. (2021) *Characterizing Urban Mobility Patterns: A Case Study of Mexico City*. Singapore, Singapore: Springer, pp. 153–170.

102. Simini, F., González, M. C., Maritan, A. & Barabási, A.-L. (2012) A universal model for mobility and migration patterns. *Nature (London)*, **484**, 96–100.

103. Liben-Nowell, D., Novak, J., Kumar, R., Raghavan, P. & Tomkins, A. (2005) Geographic routing in social networks. *Proc. Natl. Acad. Sci. USA*, **102**, 11623–11628.
104. Noulas, A., Scellato, S., Lambiotte, R., Pontil, M. & Mascolo, C. (2012) A tale of many cities: universal patterns in human urban mobility. *PLoS One*, **7**, e37027.
105. Pan, W., Ghoshal, G., Krumme, C., Cebrian, M. & Pentland, A. (2013) Urban characteristics attributable to density-driven tie formation. *Nat. Commun.*, **4**, 1961.
106. Dall, J. & Christensen, M. (2002) Random geometric graphs. *Phys. Rev. E*, **66**, 016121.
107. Estrada, E. & Sheerin, M. (2015) Random rectangular graphs. *Phys. Rev. E*, **91**, 042805.
108. Arenas, A., Díaz-Guilera, A., Kurths, J., Moreno, Y. & Zhou, C. (2008) Synchronization in complex networks. *Phys. Rep.*, **469**, 93 – 153.
109. Estrada, E. (2015) Introduction to complex networks: structure and dynamics. *Evolutionary Equations with Applications in Natural Sciences* (J. Banasiak & M. Mokhtar-Kharroubi eds), vol. 2126. *Lecture Notes in Mathematics*. Springer International Publishing, pp. 93–131.
110. Estrada, E., Hatano, N. & Benzi, M. (2012) The physics of communicability in complex networks. *Phys. Rep.*, **514**, 89 – 119.
111. Fouss, F., Saerens, M. & Shimbo, M. (2016) *Algorithms and Models for Network Data and Link Analysis*. New York: Cambridge University Press.
112. McGraw, P. N. & Menzinger, M. (2008) Laplacian spectra as a diagnostic tool for network structure and dynamics. *Phys. Rev. E*, **77**, 031102.
113. Mohar, B. (1991) The Laplacian spectrum of graphs. *Graph Theory Combin Appl.*, **2**, 871–898.
114. Mohar, B. (1997) Some applications of Laplace eigenvalues of graphs. *Graph Symmetry: Algebraic Methods Appl.*, **497**, 227–275.
115. Hänggi, P. & Marchesoni, F. (2005) Introduction: 100 years of Brownian motion. *Chaos*, **15**, 026101.
116. Group, T. F. (2016) *The Fractional Laplacian*. FL, USA: CRC Press.
117. Lischke, A., Pang, G., Gulian, M., Song, F., Glusa, C., Zheng, X., Mao, Z., Cai, W., Meerschaert, M. M., Ainsworth, M. & Karniadakis, G. E. (2020) What is the fractional Laplacian? A comparative review with new results. *J. Comput. Phys.*, **404**, 109009.
118. Tarasov, V. E. (2010) *Fractional Dynamics*. Heidelberg: Springer.
119. Zaslavsky, G. (2002) Chaos, fractional kinetics, and anomalous transport. *Phys. Rep.*, **371**, 461–580.
120. Bellman, R. (1960) *Introduction to Matrix Analysis*. New York: McGraw-Hill.
121. Michelitsch, T., Collet, B., Riascos, A. P., Nowakowski, A. & Nicolleau, F. (2018) *On Recurrence and Transience of Fractional Random Walks in Lattices*. Cham: Springer International Publishing, pp. 555–580.
122. Michelitsch, T. M., Collet, B., Nowakowski, A. F. & Nicolleau, F. C. G. A. (2016a) Lattice fractional Laplacian and its continuum limit kernel on the finite cyclic chain. *Chaos Solitons Fractals*, **82**(Supplement C), 38 – 47.
123. Abramowitz, M. & Stegun, I. A. (1970) *Handbook of Mathematical Functions*. New York: Dover.
124. Godsil, C. & Royle, G. (2001) *Algebraic Graph Theory*, vol. 207 of *Graduate Texts in Mathematics*. Berlin: Springer.
125. Estrada, E., Higham, D. J. & Hatano, N. (2009) Communicability betweenness in complex networks. *Phys. A: Stat. Mech. Appl.*, **388**, 764 – 774.
126. de Arruda, G. F., Barbieri, A. L., Rodríguez, P. M., Rodrigues, F. A., Moreno, Y. & Costa, L. F. (2014) Role of centrality for the identification of influential spreaders in complex networks. *Phys. Rev. E*, **90**, 032812.
127. Koponen, I. T. (2021) Systemic states of spreading activation in describing associative knowledge networks II: generalisations with fractional graph Laplacians and q-adjacency kernels. *Systems*, **9**, 22.
128. Estrada, E. (2021) Path Laplacians versus fractional Laplacians as nonlocal operators on networks. *New J. Phys.*, **23**, 073049.
129. Lin, Y. & Zhang, Z. (2013) Random walks in weighted networks with a perfect trap: an application of Laplacian spectra. *Phys. Rev. E*, **87**, 062140.
130. González, M. C., Hidalgo, C. A. & Barabási, A.-L. (2008) Understanding individual human mobility patterns. *Nature (London)*, **453**, 779–782.

131. Liu, Y., Wang, F., Kang, C., Gao, Y. & Lu, Y. (2014) Analyzing relatedness by toponym co-occurrences on web pages. *Trans. GIS*, **18**, 89–107.
132. Kemeny, J. G. & Snell, J. L. (1960) *Finite Markov Chains*. Princeton: VanNostrand.
133. Zhang, Z., Julaiti, A., Hou, B., Zhang, H. & Chen, G. (2011) Mean first-passage time for random walks on undirected networks. *Eur. Phys. J. B*, **84**, 691–697.
134. Gómez-Gardeñes, J. & Latora, V. (2008) Entropy rate of diffusion processes on complex networks. *Phys. Rev. E*, **78**, 065102.
135. Gray, R. M. (2006) Toeplitz and circulant matrices: a review. *Found. Trends Commun. Inf. Theory*, **2**, 155–239.
136. Watts, D. J. & Strogatz, S. H. (1998) Collective dynamics of small-world networks. *Nature (London)*, **393**, 440–442.
137. Barabási, A.-L. & Albert, R. (1999) Emergence of scaling in random networks. *Science*, **286**, 509–512.
138. Erdös, P. & Rényi, A. (1959) On random graphs, I. *Publ. Math. (Debrecen)*, **6**, 290–297.